



# ESA CONTRACT REPORT

Contract Report to the European Space Agency

## **Global Validation of ENVISAT Wind, Wave and Water Vapour Products from RA-2, MWR, ASAR and MERIS (2011-2012)**

*Author: Saleh Abdalla*

Final report for ESA contract 21519/08/I-OL (CCN1)

European Centre for Medium-Range Weather Forecasts  
Europäisches Zentrum für mittelfristige Wettervorhersage  
Centre européen pour les prévisions météorologiques à moyen terme



Series: ECMWF ESA Project Report Series

A full list of ECMWF Publications can be found on our web site under:

<http://www.ecmwf.int/publications/>

Contact: [library@ecmwf.int](mailto:library@ecmwf.int)

© Copyright 2013

European Centre for Medium Range Weather Forecasts  
Shinfield Park, Reading, Berkshire RG2 9AX, England

Literary and scientific copyrights belong to ECMWF and are reserved in all countries. This publication is not to be reprinted or translated in whole or in part without the written permission of the Director. Appropriate non-commercial use will normally be granted under the condition that reference is made to ECMWF.

The information within this publication is given in good faith and considered to be true, but ECMWF accepts no liability for error, omission and for loss or damage arising from its use.

Contract Report to the European Space Agency

**Global Validation of ENVISAT  
Wind, Wave and Water Vapour Products  
from RA-2, MWR, ASAR and MERIS  
(2011-2012)**

*Author: Saleh Abdalla*

*Final report for ESA contract 21519/08/I-OL (CCN1)*

European Centre for Medium-Range Weather Forecasts  
Shinfield Park, RG2 9AX, Reading, UK.

March 2013



## Table of Contents

<b>Summary</b> .....	<b>1</b>
<b>Abbreviations</b> .....	<b>2</b>
<b>Major changes and events</b> .....	<b>4</b>
<b>I Radar altimeter - 2 (RA-2) and Microwave radiometer (MWR)</b> .....	<b>7</b>
I.1 Introduction .....	9
I.2 RA-2 and MWR data processing.....	10
I.3 FD RA-2 data reception .....	10
I.4 RA-2 radar backscatter and surface wind speed.....	12
I.5 RA-2 KU-band significant wave height.....	15
I.6 RA-2 S-band significant wave height.....	18
I.7 MWR products .....	18
I.8 Conclusions .....	24
<b>II Advanced Synthetic Aperture Radar (ASAR) wave mode products</b> .....	<b>25</b>
II.1 Introduction .....	27
II.2 ASAR data processing.....	27
II.3 ASAR level 1B product.....	29
II.4 ASAR WM Level 2 product.....	32
II.5 Assimilation of ASAR Wave Mode Level 2 product.....	35
II.6 Conclusions .....	39
<b>III Medium Resolution Imaging Spectrometer (MERIS) Water vapour product</b> .....	<b>41</b>
III.1 Introduction .....	43
III.2 MERIS data processing for monitoring.....	43
III.3 MERIS Water vapour product.....	44
III.4 Assimilation of MERIS TCWV .....	47
III.5 Conclusions .....	47
<b>Acknowledgments</b> .....	<b>48</b>
<b>References</b> .....	<b>48</b>



## Summary

ENVISAT Fast Delivery (FD) surface wind speed and significant wave height (SWH) products from the Radar Altimeter (RA-2) instrument, wet tropospheric correction (WTC) and total column water vapour (TCWV) products from the Microwave Radiometer (MWR) instrument, wave mode spectra (both Level 1b and Level 2) from the Advanced Synthetic Aperture Radar (ASAR) instrument and TCWV product from the Medium Resolution Imaging Spectrometer (MERIS) instrument have been monitored and validated against the corresponding parameters from ECMWF Integrated Forecast System (IFS), in-situ buoy and platform instruments and other satellites (specifically: Jason-1 and Jason-2). This report assesses the quality of related ENVISAT products during the last few years with emphasis on the years 2011-2012.

In general, the FD RA-2 products are of good quality. The wind speed product is quite good especially after resolving the issue of capping wind speed at 21.4 m/s with the introduction of RA-2 processing chain IPF Version 6.02L04 on 1 February 2010. The implementation of IPF 6.02L04 resulted in an unbiased Ku-band SWH product but, unfortunately, slightly downgraded product in terms of the standard deviation. The S-band SWH product is not valid anymore due to the failure of the S-band Altimeter in January 2008. Compared to the model, the MWR products are of good quality after filtering out the ice and land contaminated observations.

FD ASAR Wave Mode Level 1b (ASA\_WVS\_1P) product as inverted using the Max-Planck Institut für Meteorologie (MPIM) scheme agrees well with the wave model counterpart in terms of all integrated parameters used for the comparison. ASAR Wave Mode Level 1b product has been assimilated operationally at ECMWF since 1 February 2006. On the other hand, Wave Mode Level 2 (ASA\_WVW\_2P) product agrees well with wave model in terms of swell SWH and mean period. Irrespective of a rather recent improvement of the product in October 2008, the agreement is not so good for spectral peakedness factor and the directional spread. There was no noticeable change in the ASAR Wave Mode products during the last two years. Further work was carried out in order to assimilate ASAR Wave Mode Level 2 product with limited success. It seems that further investigation and/or product improvement are needed.

Slight improvement in the quality of MERIS TCWV product was witnessed after the operational implementation of the MERIS IPF Version 6.04 on 03 November 2011. The change list includes, among others, a new algorithm for water vapour retrieval over land. The differences between MERIS and the model are still relatively high. However, the product is quite good over land where similar products are lacking. MERIS TCWV product has been assimilated operationally in the ECMWF operational atmospheric model since early September 2009.

The change of ENVISAT orbit in October 2010 did not have any impact on any of the products considered here. Unfortunately, communication with ENVISAT was permanently lost on 8 April 2012 and the end-of-mission was declared few weeks later. Although this declaration put an end to a highly productive era, the invaluable data collected during the 10-year mission life will continue to be of great use by the wind and wave community. At ECMWF, in particular, the data will continue to be used for the verification of model upgrades as well as for the future reanalysis efforts.

## Abbreviations

AN .....	Analysis
ASAR .....	Advanced Synthetic Aperture Radar
BUFR .....	Binary Universal Form for the Representation of meteorological data
ECMWF .....	European Centre for Medium-Range Weather Forecasts
ECWAM.....	ECMWF wave model
ENVISAT.....	Environmental Satellite
ERS.....	European Remote Sensing satellite
FD.....	Fast Delivery product
FDGDR .....	Fast Delivery Geophysical Data Record
FDMAR.....	Fast Delivery Marine Abridged Records Product
FG.....	First guess
GTS .....	Global Telecommunication System
IPF .....	Instrument Processing Facility
MERIS.....	MEdium Resolution Imaging Spectrometer
MPIM .....	Max-Planck Institut für Meteorologie
MWD.....	Mean wave direction
MWP .....	Mean wave period
MWR.....	MicroWave Radiometer
NH .....	Northern Hemisphere extra-tropics (north of latitude 20°N)
NRT.....	Near real time
NWP .....	Numerical weather prediction
PF-ASAR .....	ASAR Processing Facility
QC .....	Quality control



QWG ..... Quality Working Group

RA ..... ERS Radar Altimeter

RA-2 ..... ENVISAT Radar Altimeter-2

SH..... Southern Hemisphere extra-tropics (south of latitude 20° S)

SI ..... Scatter Index

SWH..... Significant wave height

TCWV ..... Total column water vapour

UTC..... Coordinated Universal Time

WAM..... Wave model

WDS ..... Wave directional spread

WPF..... Wave spectral peakedness factor of Goda

WTC..... Wet tropospheric correction

## Major changes and events

The main results of the validation of ENVISAT Fast Delivery (FD) products of Radar Altimeter-2 (RA-2) and Microwave Radiometer (MWR) Level 2, Advanced Synthetic Aperture Radar (ASAR) Wave Mode (WM) Level 1b and Level 2, and Medium Resolution Imaging Spectrometer (MERIS) Level 2 (water vapour product only) over the last few years are presented here. The following major changes and events during the last few years are known to have effect on the interpretation of the validation results:

- 30 October 2007: The implementation of the processing chain of PF-ASAR 4.05.
- 18 January 2008: The loss of RA-2 S-band.
- 3 June 2008: The advection numerical scheme of the wave model was changed.
- 30 September 2008: Changes to the physics of the atmospheric model.
- 10 March 2009: The operational assimilation of Jason-2 significant wave height replacing that of Jason-1. A change in the treatment of some atmospheric observations impacted the model water vapour.
- 8 June 2009: The re-introduction of the assimilation of Jason-1 significant wave height.
- 8 September 2009: Wave model change to account for the wave damping in the wind input source term. The operational assimilation of MERIS TCWV (over land only) in the ECMWF atmospheric model.
- 10 November 2009: Revised significant wave height bias correction in the wave model.
- 26 January 2010: The high resolution (T1279) atmospheric model with a resolution of 16 km. The increase of number of frequency and direction bins in the wave model.
- 1 February 2010: The implementation of the RA-2 IPF 6.02L04 which affected significant wave height, backscatter, wind speed and water vapour products.
- 22 March 2010: Revised significant wave height bias correction to account for the impact of IPF 6.02L04 on model wave height.
- 1 April 2010: Assimilation of Jason-1 significant wave heights was halted.
- 19 October 2010: MWR anomaly caused the rain flag in the RA-2 products to be set. This caused the rejection of most of RA-2 products. The anomaly was sorted out within few days during the period of ENVISAT orbit reconfiguration.
- 22-26 October 2010: ENVISAT orbit was lowered by 17 km. The new orbit has a “repeat cycle” of about 30 days. As a precautionary measure, all ENVISAT products were not allowed to be assimilated in IFS since 21 October
- 9 November 2010: Implementation of IFS Cycle 36R4 which contains several physical and numerical changes.

- 27 November 2010: The start of the leapfrog experiment of ASAR.
- 2 December 2010: Assimilation of RA-2 significant wave height resumed.
- 3 November 2011: Implementation of MERIS IPF Ver. 6.04.
- 15 November 2011: Implementation of IFS Cycle 37R3 which includes changes to the treatment of surface roughness, cloud and convection.
- 8 Apr. 2012: Loss of communications with ENVISAT. End-of-mission was declared few weeks later.

All ECMWF Integrated Forecast System (IFS) model changes are summarised at:

[http://www.ecmwf.int/products/data/technical/model\\_id/index.html](http://www.ecmwf.int/products/data/technical/model_id/index.html)



# **I Radar altimeter - 2 (RA-2) and Microwave radiometer (MWR)**



## I.1 Introduction

RA-2 is a dual-frequency altimeter operating on both Ku- and S-band. It was derived from the RA of the ERS satellite series, providing improved measurement performance and new capabilities. The main objectives of the RA-2 are the high-precision measurements of the time delay, the power and the shape of the reflected radar pulses for the determination of the satellite height and the Earth surface characteristics. RA-2 transmits radio frequency pulses that propagate at approximately the speed of light. The time elapsed from the transmission of a pulse to the reception of its echo, reflected from the surface of the Earth, is proportional to the altitude of the satellite. The magnitude and shape of the echoes contain information on the characteristics of the surface that caused the reflection. Operating over oceans, these measurements are used to determine the ocean surface topography, thus supporting studies of ocean waves, marine surface winds, circulation, bathymetry, gravity anomalies and marine geoid characteristics. Furthermore, the RA-2 is able to map and monitor sea ice and polar ice sheets. The product to be validated here is the Fast Delivery Marine Abridged Records Product (FDMAR). Specifically, the backscatter coefficient, surface wind speed, Ku-band significant wave height (SWH) and S-band SWH are validated.

MWR is a dual-channel nadir-pointing radiometer, operating at frequencies of 23.8 GHz and 36.5 GHz. The main objective of the MWR is the measurement of the integrated atmospheric water vapour column and cloud liquid water content, as correction terms for the radar altimeter signal. In addition, MWR measurement data are useful for the determination of surface emissivity and soil moisture over land, for surface energy budget investigations to support atmospheric studies, and for ice characterization. To measure the strength of the weak water-vapour emission-line at 22 GHz, the frequencies 23.8 GHz and 36.5 GHz are optimally selected in order to eliminate the microwave radiation emitted by the Earth surface. The two products to be verified are the total column water vapour (TCWV) and the wet tropospheric correction (WTC) available in FDMAR product.

The European Centre for Medium-Range Weather Forecasts (ECMWF) monitors routinely the quality of the wind and wave products from RA-2 since an early stage of commissioning phase data dissemination on 18 July 2002. The monitoring is based on the data processed in near real time (NRT) provided by ESA. Radar backscatter coefficient ( $\sigma^0$ ), surface wind speed and Ku- and S-band SWH products from the RA-2 instrument and WTC and TCWV products from the MWR instrument are among the parameters monitored and validated against the ECMWF model products and, for wind and wave products, against the in-situ buoy and platform observations available through the Global Telecommunication System (GTS) as well as the ERS-2 RA products. When possible, a combination of all of the observation sources (multiple-collocation) is also used for validation. It must be stressed that the number of in-situ observing stations is very limited (few-several 10's) and most of them are located in the Northern Hemisphere (NH) around the North American and European coasts. The exceptions are few buoys in the Tropics, mainly around Hawaii, and off the South African coasts in the Southern Hemisphere (SH). Therefore, any validation against in-situ data mainly reflects the quality of the products in the NH.

The aim of the validation is to assess and monitor the quality of those products. The Ku-band SWH product is of significant importance as it is assimilated in the operational forecasting system at ECMWF. For proper validation, the observations and the model results should be of comparable scales. The model scale is much larger than the scale of the altimeter observations. Therefore, an averaging process is used to form altimeter and MWR super-observations of comparable scales as the model. The super-observations are collocated with the model and the in-situ (if applicable) data. The main results of the validation over the last few years are presented here.

Results of the routinely global monitoring and validation of ENVISAT RA-2 wind and wave products as well as MWR WTC and TCWV products are summarised in form of monthly reports. These reports are available online at: <http://earth.esa.int/pcs/envisat/ra2/reports/ecmwf/>

## **I.2 RA-2 and MWR data processing**

The validation is based on FDMAR (Fast Delivery Marine Abridged Record) which is a sub-set of the Fast Delivery Geophysical Data Record (FDGDR) product produced in NRT. The data files are retrieved in BUFR (Binary Universal Form for the Representation of meteorological data) format from two ftp sites at Kiruna and ESRIN. The raw data product is collected for 6-hourly time windows centred at synoptic times (00, 06, 12 and 18 UTC). For proper validation, the observations and the model results should be of comparable scales. As the model scale ( $\sim 70$  km) is much larger than the scale of an individual 1 Hz altimeter observation ( $\sim 7$  km), the latter needs to be averaged. Therefore, the stream of altimeter data is split into short observation sequences each consisting of 11 individual (1-Hz) observations. A quality control procedure is performed on each short sequence. Erratic and suspicious individual observations are removed and the remaining data in each sequence are averaged to form a representative super-observation, providing that the sequence has enough number of "good" individual observations (at least 7). The super-observations are collocated with the model and the in-situ (if applicable) data. The raw data pass the quality control and the collocated data are then investigated to derive the conclusions regarding the data quality. It is important to recall that the Ku-band SWH product is of significant importance as it is assimilated in the operational forecasting system at ECMWF since 21 October 2003. The details of the method used for data processing is an extension to the method used for ERS-2 RA analysis and described in Abdalla and Hersbach (2004).

## **I.3 FD RA-2 data reception**

FD RA-2 data reception during year 2011 was quite good. However, there were quite a number of data gaps. Fig. (I.1) represents the data reception during the relaxed cut-off condition of the Delay Cut-off (DCDA) the ECMWF IFS model configuration (8~14-hour delay). The products are considered missing if they are delayed beyond the cut-off limit. Therefore, some of the gaps may just represent this fact.



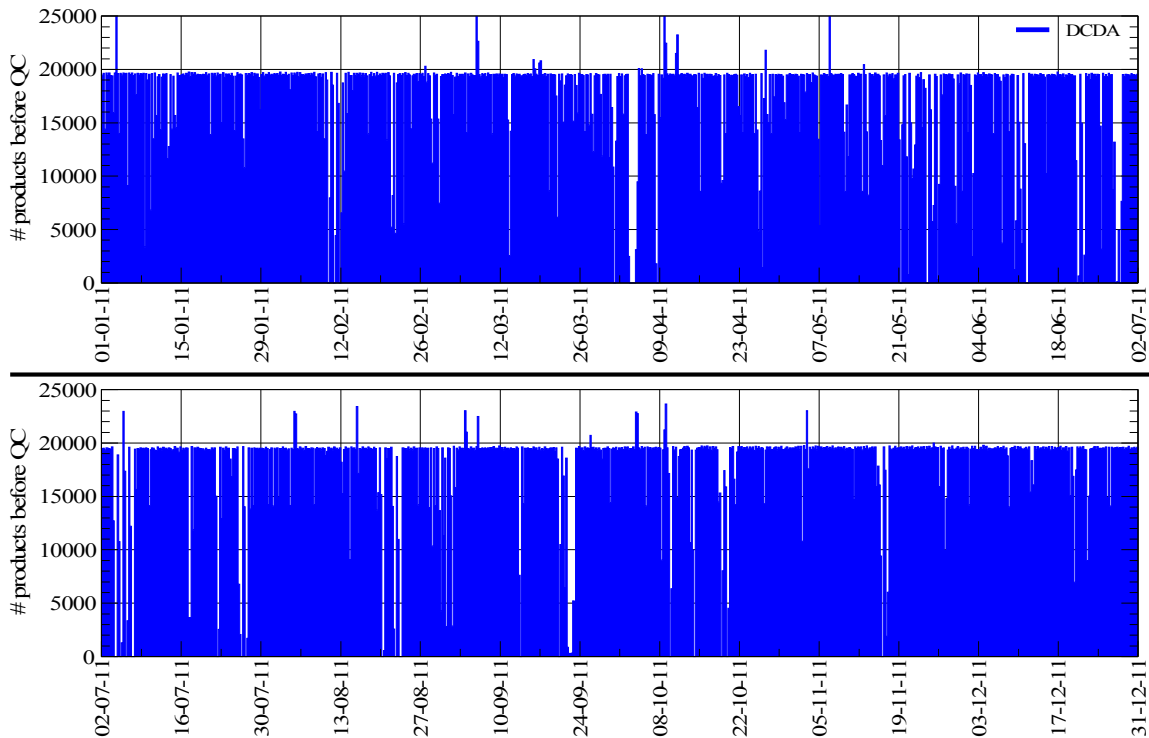


Figure I.1: Total Operational Data Reception of RA-2 Data in 2011.

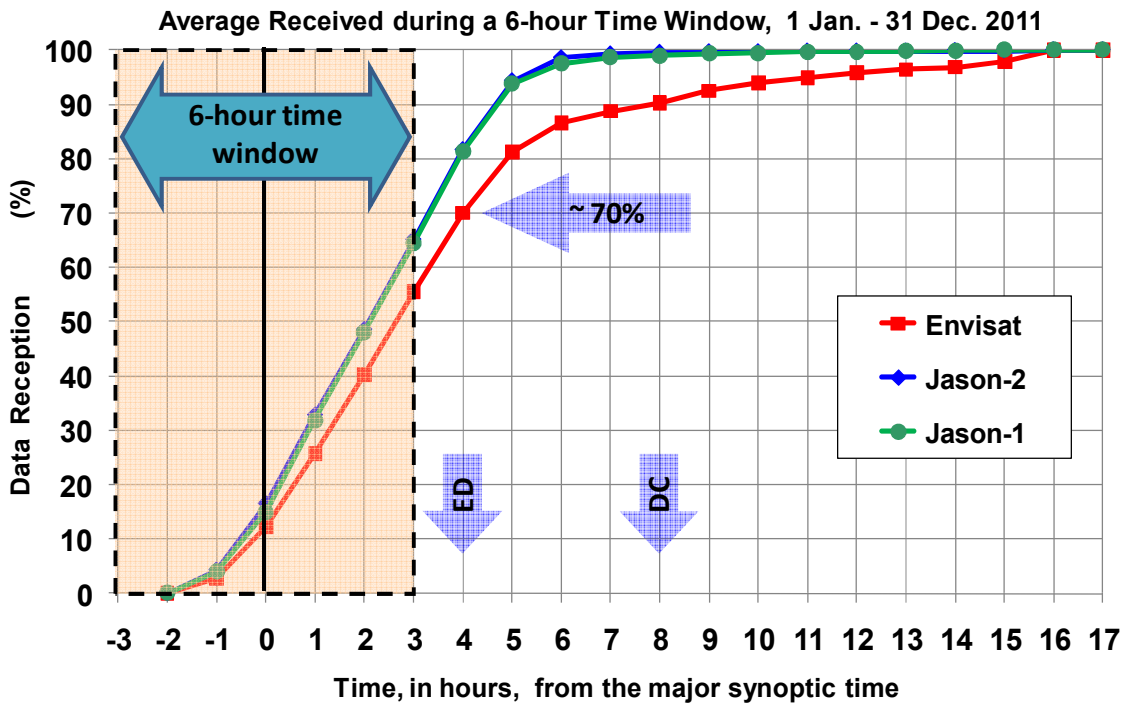


Figure I.2: Amount of operational data reception of RA-2 data in 2010 as a function of waiting time. The cut-off for the “Early Delivery” (ED) suite and the critical cut-off for the “Delayed Cut-off” (DC) suite are indicated. The same results from Jason-1/2 are also presented.

In order to quantify the timeliness of the arrival of the RA-2 products, the products within each 6-hour time window (centred at 00, 06, 12 and 18 UTC) were discriminated based on their arrival time measured from the centre of the window. The accumulative amount of data received at each hour is averaged over a long period of time (e.g. a full year). Fig. (I.2) shows the average accumulated amount (normalised by the total amount of data received at the end of 48 hours) of data received for all 6-hour time windows during 2011 as a function of the time since the middle of the time windows. The official ECMWF forecasts are issued from the “Early Delivery (ED)” cut-off, which is 1 hour after the close of the 6-hour window. This makes 4 hours from the centre of the analysis window. RA-2 products available for assimilation at this cut-off time is about 70% of the total received after waiting long enough. This is a slight improvement compared to the 68% of 2010 and 65% of 2009. Although this is considerable amount of data, better performance can be achieved as can be seen in Fig. (I.2) for Jason-1 and Jason-2 products (about 80%). For the minimum cut-off of the DCDA suite (5 hours after the end of the window), about 90% of the data are available for analysis. This, again, shows that there is room for improvement as Jason-1/2 data products were almost fully received. It seems that delivering the data through the GTS, which is the medium used for delivering Jason-1/2 data, does not help much to improve this.

#### I.4 RA-2 radar backscatter and surface wind speed

In general, the FD RA-2 Ku band backscatter coefficient ( $\sigma^\circ$ ) behaves as expected. The monthly mean values of  $\sigma^\circ$  since May 2003 are plotted in panel (a) of Fig. (I.3). One can notice that the monthly mean Ku-band  $\sigma^\circ$  values vary within a narrow band between 10.9 and slightly above 11.2 dB. The monthly mean of S-band  $\sigma^\circ$  values are shown on the same plot. The S-band has been declared permanently lost since early January 2008. The time series of the S-band is rather stable except for two events. There was a jump of about 0.6 dB between November and December 2003. The jump coincides with the implementation of the IPF Version 4.56 processing chain on the 26 November 2003. The second event was the drop in the Side B S-band transmission power as can be clearly seen in Fig. (I.2) for May and June 2006. For comparison, Jason-1 and Jason-2 radar altimeter monthly mean  $\sigma^\circ$  values from both Ku- and C-Bands are also plotted in Fig. (I.3). Apart from the fact that Jason mean backscatter values are higher than those of ENVISAT, they are all run more or less parallel to each other. However, it seems that Jason-1 mean values suffer gradual de-crease.

At the end of 2009, there was an apparent drop in the backscatter values of all altimeters. This can be clearly seen in panel (b) of Fig. (I.3) which shows the 1-year running averages of the mean  $\sigma^\circ$  values to filter out all seasonal and shorter scale fluctuations. Therefore, a drop in RA-2 Ku-band mean values of about 0.15 dB can be clearly seen. However, this value is about twice those suffered by the Ku-band altimeters (about 0.08 dB) onboard Jason-1/2. The drop in the Jason-1/2 C-bands is about 0.05 dB. The possible reasons for this drop are not clear but the issue is still under investigation. It should be noted that, the RA-2 higher drop compared to Jason-1/2 is due to the implementation of the IPF Ver. 6.02L04 on 1 February 2010 which resulted in slightly lower values of backscatter. This added further to the drop of concern towards the end of 2009. Another, yet minor, reason for that is due to the fact that ENVISAT reaches much higher latitudes where the atmospheric conditions are different from low-mid latitudes covered by Jason-1/2.

Collocated pairs of RA-2 super-observation and the analysed (AN) ECMWF model wind speeds are plotted as a density scatter plot in Fig. (I.4) for the whole globe over a period of one year from 1 January to 31 December 2011. On the other hand, Fig. (I.5) shows a similar plot comparing the altimeter winds against in-situ (buoy) data for the same period. In general, RA-2 wind speed data are in good agreement with the model and buoy data.

The global wind speed bias (defined as the RA-2 minus the model or the buoy) is about 0.29 m/s. On the other hand, the RA-2 wind speeds are lower than the buoys by about 0.11 m/s. One needs to keep in mind that most of the in-situ (buoy or platform) instruments are located around North America and Europe. Therefore, the comparison against in-situ observations mainly reflects the quality of the wind speed product in the NH (and to less extent in the Tropics). The global RA-2 wind speed scatter index (SI, defined as the standard deviation of difference divided by the mean of the model or the buoy) is about 14% when compared against the model and about 17% compared to the buoys.

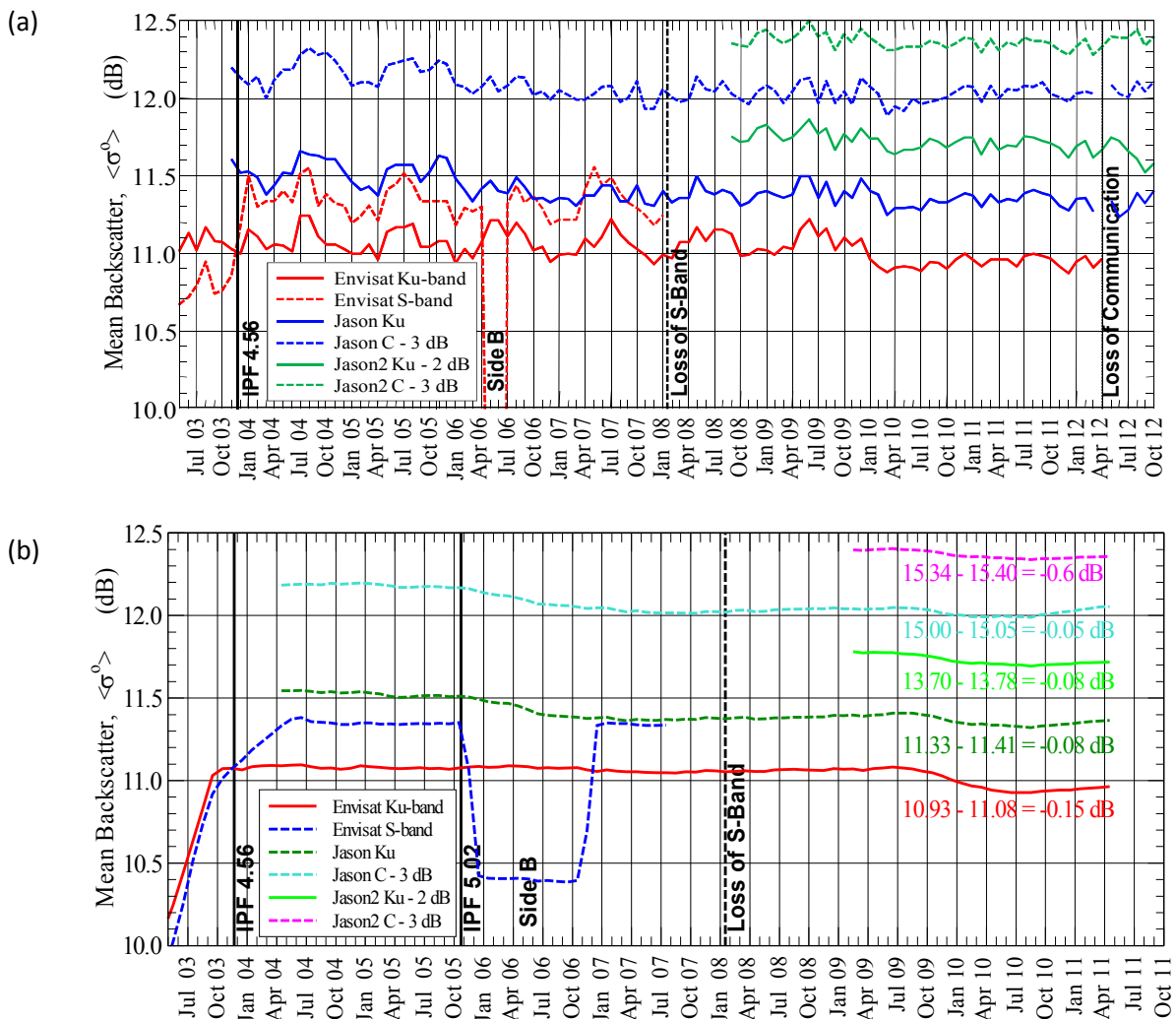


Figure I.3: Monthly global mean backscatter coefficient of Ku- and S-band altimeters after quality control. Jason-1 and Jason-2 Ku- and C-band mean backscatter values are also shown for comparison. (a) Individual monthly means, (b) 12-month running average of the monthly means. Note that panel the x-axis of Panel (b) ends earlier than that of Panel (a).

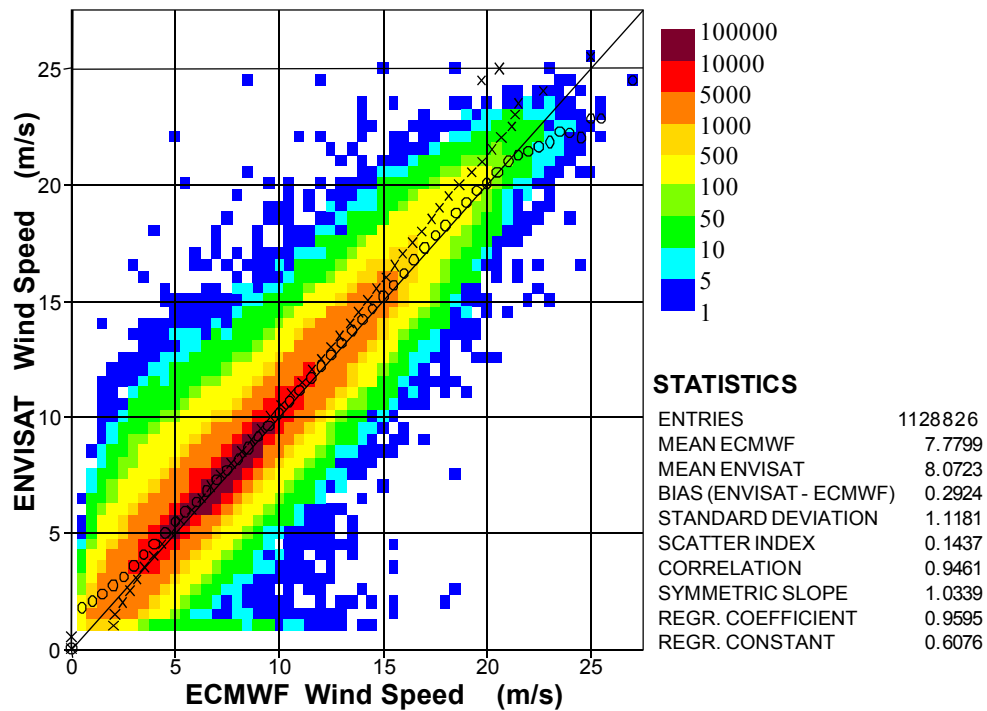


Figure I.4: Global comparison between RA-2 and AN ECMWF model wind speed values during the period from 1 January 2011 to 31 December 2011.

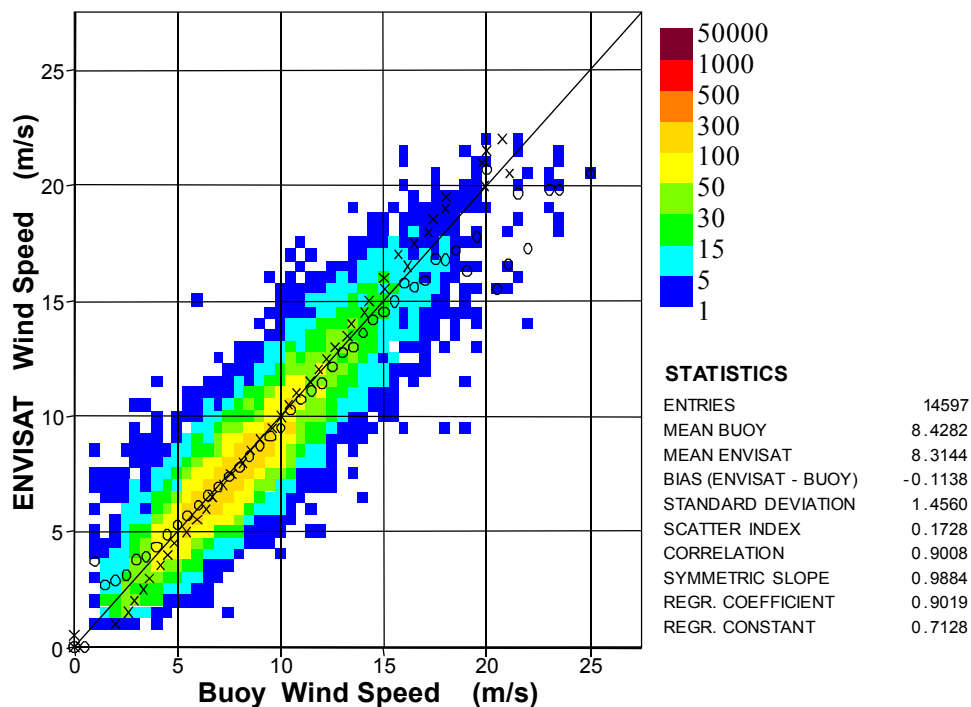


Figure I.5: Global comparison between RA-2 and in-situ wind speed values during the period from 1 January 2011 to 31 December 2011 (mainly in the NH).

The time series of weekly bias and standard deviation of the difference (SDD) between RA-2 and model AN wind speeds since late 2003 are shown in panel (a) of Fig. (I.6) and during the last 4 years in panel (b) of Fig. (I.6). The major altimeter related events and the ECMWF model changes are shown as well. One can clearly see the seasonal variation of the bias. After the implementation of IPF Version 5.02 (October 2005), the seasonal variation is much suppressed especially in the NH and the Tropics (not shown). For example, the range of variation in the NH reduced from about 1.3 m/s (-0.9 to 0.4 m/s) to about 0.9 m/s (-0.2 to 0.7 m/s). The global range of variation reduced by half from about 0.4 m/s to about 0.2 m/s (Fig. I.6). The implementation of IPF 6.02L04 on 1 February 2010 resulted in slightly higher bias than before due to the removal of the cap ( $\sim 21.4$  m/s) which was imposed before. On the other hand there was an increase in bias and SDD just after the orbit change. This lasted for a couple of days only and the statistics returned back to normal. There was no obvious reason for this. However, M. Roca (personal communication, 2010) claimed that this may be due to the colder than normal conditions of the platform as most of the instruments on-board ENVISAT were switched off during the orbit changing manoeuvres. Of course it is not possible to prove or disprove this conjecture easily.

Wind speed from RA-2 is not assimilated in the ECMWF models. The main reason for that is the existence of the overwhelming amount of scatterometer winds making the altimeter wind observations of very minimal impact, if any. However, the altimeter wind speed observations are playing a very important role as an independent source of data which can be used to assess the ECMWF model developments as can be seen, for example, in Fig. (I.6).

## **I.5 RA-2 KU-band significant wave height**

Ku-band SWH product is characterised by stable performance and good quality since the start of the mission. Collocated SWH pairs of RA-2 super-observation and the first-guess (FG) WAM model are plotted as a density scatter plot in Fig. (I.7) for the whole globe over the whole year of 2011. The RA-2 used to overestimate SWH values globally by about 4% ( $\sim 10$ - $12$  cm). The IPF 6.02L04 (February 2010) brought the bias down to very close to zero ( $\sim 0.5\%$  or  $\sim 4$  cm). Similar results can be obtained from the comparison against in-situ buoy data as shown in Fig. (I.8) for the same period. It should be stressed here that buoy observations are mainly in the NH.

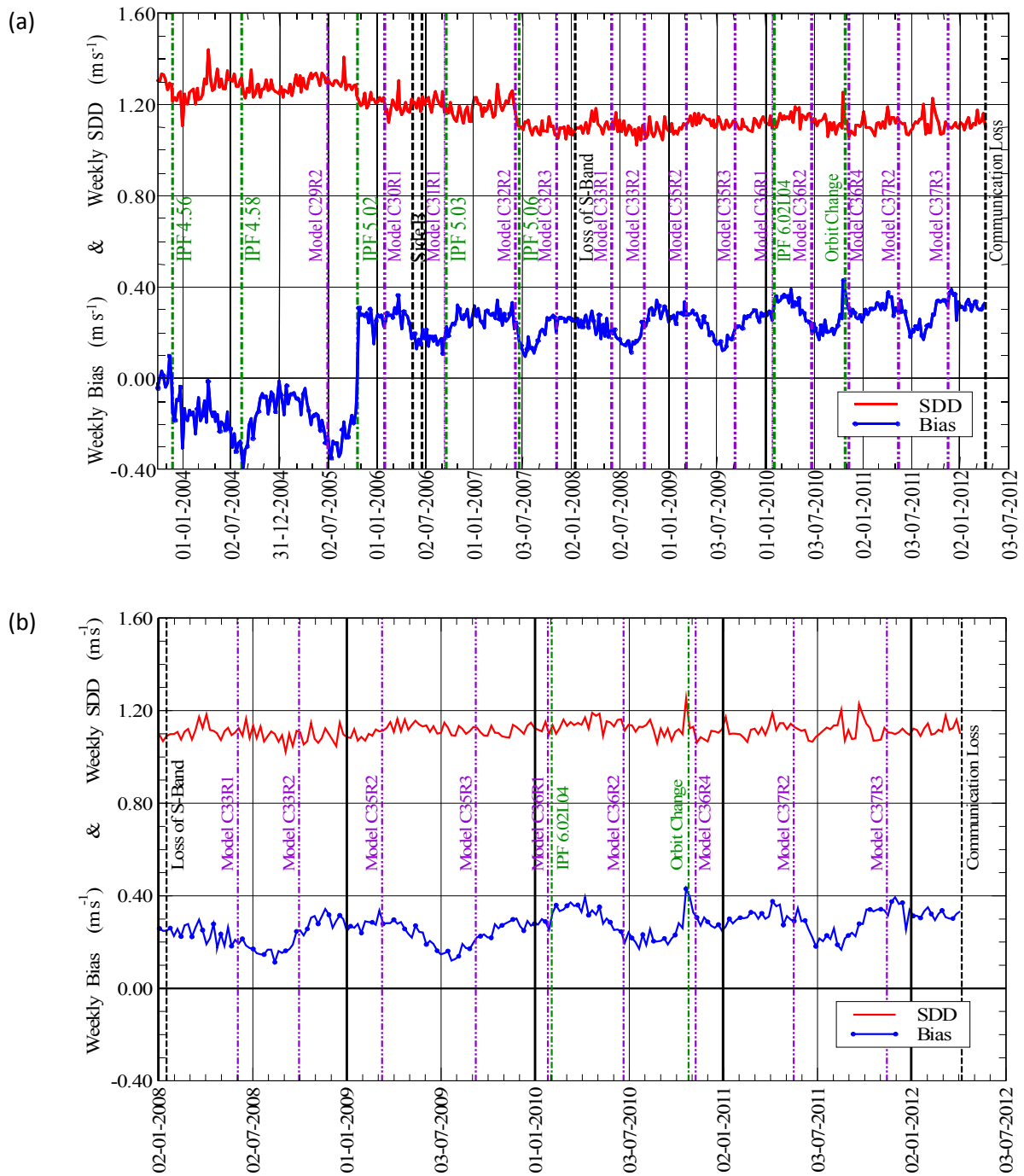


Figure I.6: Time series of weekly wind speed bias ( $\text{m/s}$ ) and standard deviation of difference (SDD) between RA-2 and ECMWF model AN since late 2003 (a) and during the last 4 years (b).

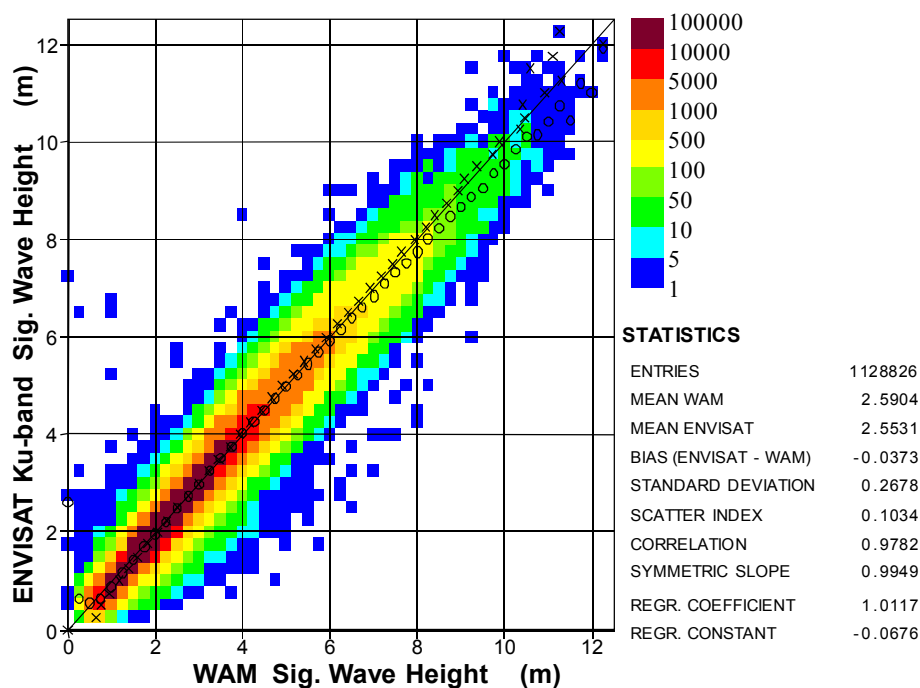


Figure 1.7: Global comparison between RA-2 Ku-band and WAM wave model SWH FG values during the period from 1 January 2011 to 31 December 2011.

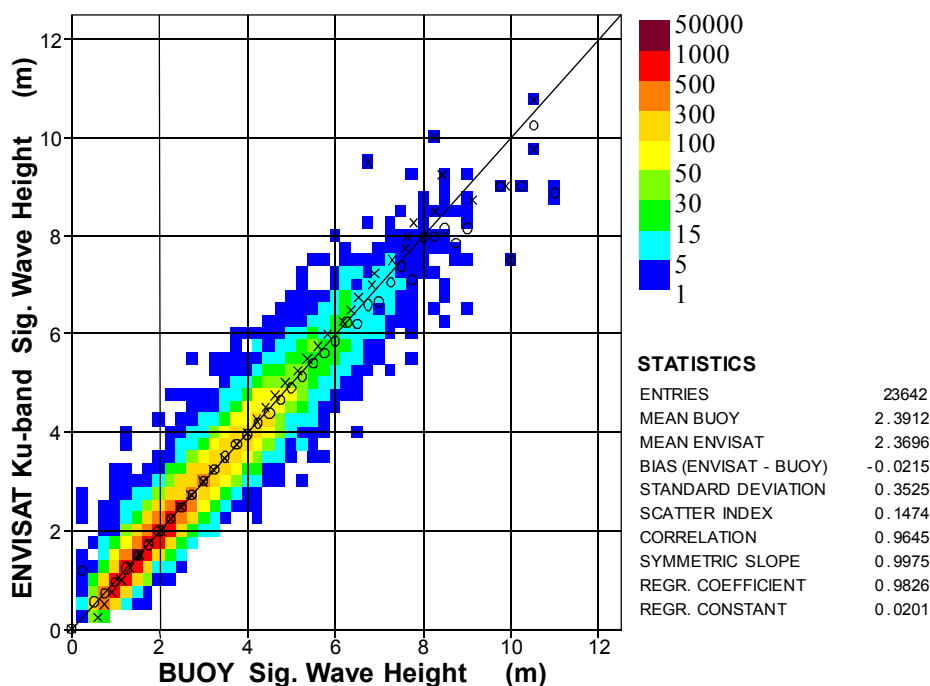


Figure 1.8: Global comparison between RA-2 Ku-band and in-situ SWH values during the period from 1 January 2011 to 31 December 2011 (mainly in the NH).

The time series of weekly bias and SDD between RA-2 and model FG SWH since late 2003 are shown in panel (a) of Fig. (I.9) and during the last 4 years are shown in panel (b). Significant model or RA-2 processing changes are plotted as well so that the correspondence between those events and the change in statistics is clearly seen. Fig. (I.9), or the cross-verification of model and altimeter time series represents a valuable tool to detect and assess changes on both sides. Fig. (I.9) represent the time series for model or altimeter processing improvement (or degradation) by following the trend of the SDD over time. For example; RA-2 side B operation during May and June 2006 caused one of the most significant impacts on the statistics. The abrupt reduction in SWH bias and SDD between RA-2 and ECMWF model FG during the period when RA-2 was configured to side B cannot be missed. Another prominent change is the implementation of IPF 6.02L04. The bias clearly reduced by about 12 cm due to this change. It also led to a slight increase in SDD (see Abdalla, 2011). The impact of the revised bias corrections of the altimeter SWH in November 2009 and March 2010 can also be clearly seen in Fig. (I.9).

## I.6 RA-2 S-band significant wave height

“Envisat RA-2 (A-Side) S-band transmission power suddenly dropped at 23:23:40 UTC on 17 January 2008”. All S-band products are no longer valid since then. This was declared to be a permanent failure by ESA.

Before the failure, the quality of S-band wave height product used to be of acceptable quality after some quality control procedure to filter out the observations contaminated by the “S-band Anomaly” (which disappeared shortly before the permanent failure of the S-band altimeter).

## I.7 MWR products

Two MWR products are monitored and validated: the total column water vapour (TCWV) and the wet tropospheric correction (WTC). Both parameters are functions of the 23.8-GHz (TB23) and 36.5-GHz (TB36) brightness temperatures and wind speed. ECMWF atmospheric model computes TCWV as one of its standard output products. Model WTC can be calculated from pressure, temperature and humidity fields. For the validation of the MWR products analysis (AN) model fields are used.

Collocated TCWV pairs of MWR super-observation and the ECMWF model AN are plotted as density scatter plots in Fig. (I.10) for the whole globe for one year period from 1 January to 31 December 2011. It should be stressed that strict quality control based on Altimeter products was implemented to remove a large number of outliers resulted from sea-ice contamination. Apart from a handful of outliers, the MWR TCWV observations agree very well with the model for both periods. Some of outliers happen very close to the coast, which suggests possible land contamination. The agreement is very good with a scatter index (SDD normalised by the mean value of the model) of less than 8% and a correlation in excess of 99%. The implementation of the IPF 6.02L04 RA-2 processing chain in February 2010 eliminated the long-lasting issue of the scatter plot hump below the main cloud between model TCWV values of 15 and 20 kg/m<sup>2</sup> (Abdalla, 2011).



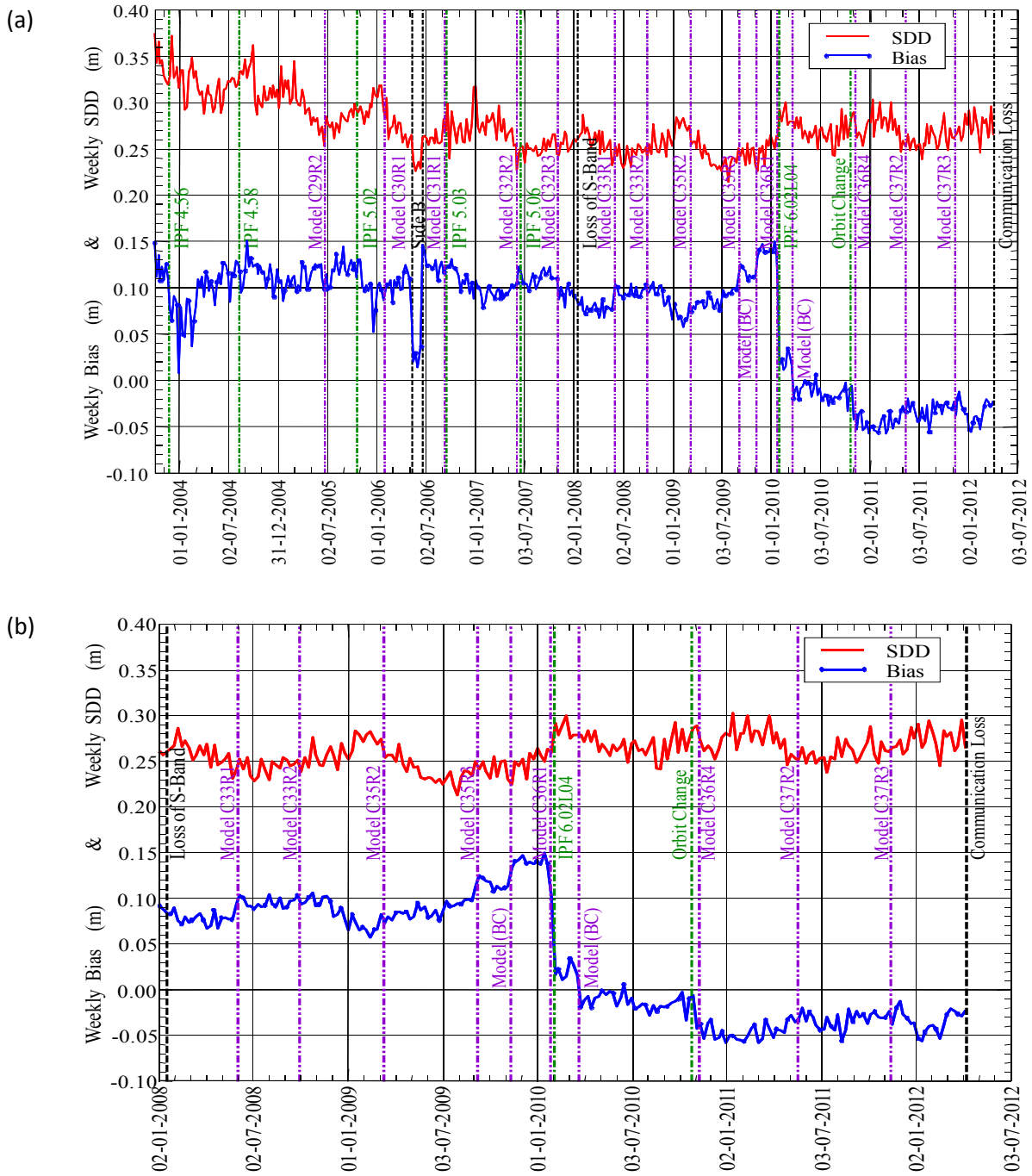


Figure I.9: Time series of weekly SWH bias and standard deviation of difference (SDD) between RA-2 Ku-band and WAM model FG since late 2003 (a) and during the last 4 years (b).

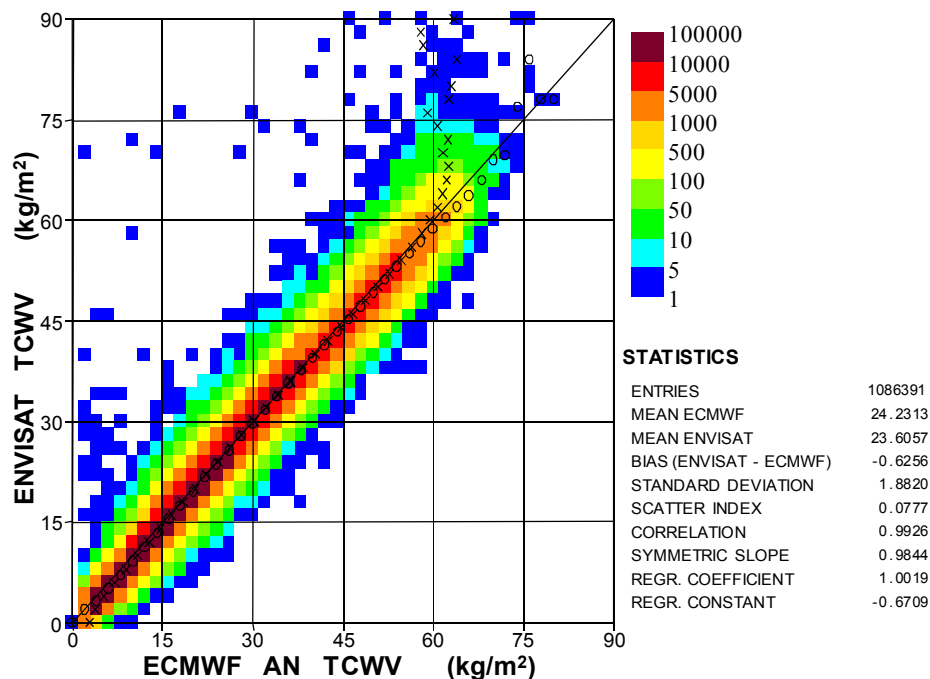


Figure I.10: Global comparison between MWR and ECMWF model AN TCWV values during the period from 1 January 2011 to 31 December 2011.

The time series of weekly bias and SDD between MWR and ECMWF model TCWV since late 2003 are shown in panel (a) of Fig. (I.11) while the time series for the last 4 years are shown in panel (b). Fig. (I.11) suggests that there is a seasonal cycle in the bias during the last 5 years or so. However, it was not possible to neither prove nor disprove the genuine existence of this seasonal cycle. The other remark is the drier nature of the MWR observations compared to the model values.

The impact of various IPF instrument processing chains, like IPF Ver. 4.56 (November 2003) and IPF Ver. 6.02L04 (February 2010) and model changes like model Cycle 32R2 (November 2007), Cycle 35R2 (March 2009) and Cycle 36R4 (November 2010) can be clearly seen in Fig. (I.11). The MWR TCWV product is used to assess the ECMWF atmospheric model changes as an independent source of data. For example, the significant improvements, both the random and the systematic errors, of the model Cycle 36R4 were very obvious when compared against MWR products. The improvement of the MWR products due to the implementation of IPF6.02L04 can also be detected from the time series plot (Fig. I.11). The elimination of the “hump” mentioned earlier was certainly one of the reasons for this improvement.

Collocated WTC pairs of MWR super-observation and the ECMWF model AN are plotted as density scatter plots in Fig. (I.12) for the whole globe for the one year period from 1 January to 31 December 2011. Similar to the TCWV product, the majority of the MWR WTC observations agree very well with the model counterpart. The agreement is very good with scatter index of slightly above 9% and a correlation coefficient of slightly less than 99%. However, there are quite a number of outliers as well. The outliers are mainly associated with model low values (less than ~10 cm). As for the case of TCWV, the major parts of the outliers occur near the ice edges. Therefore, stricter QC criteria

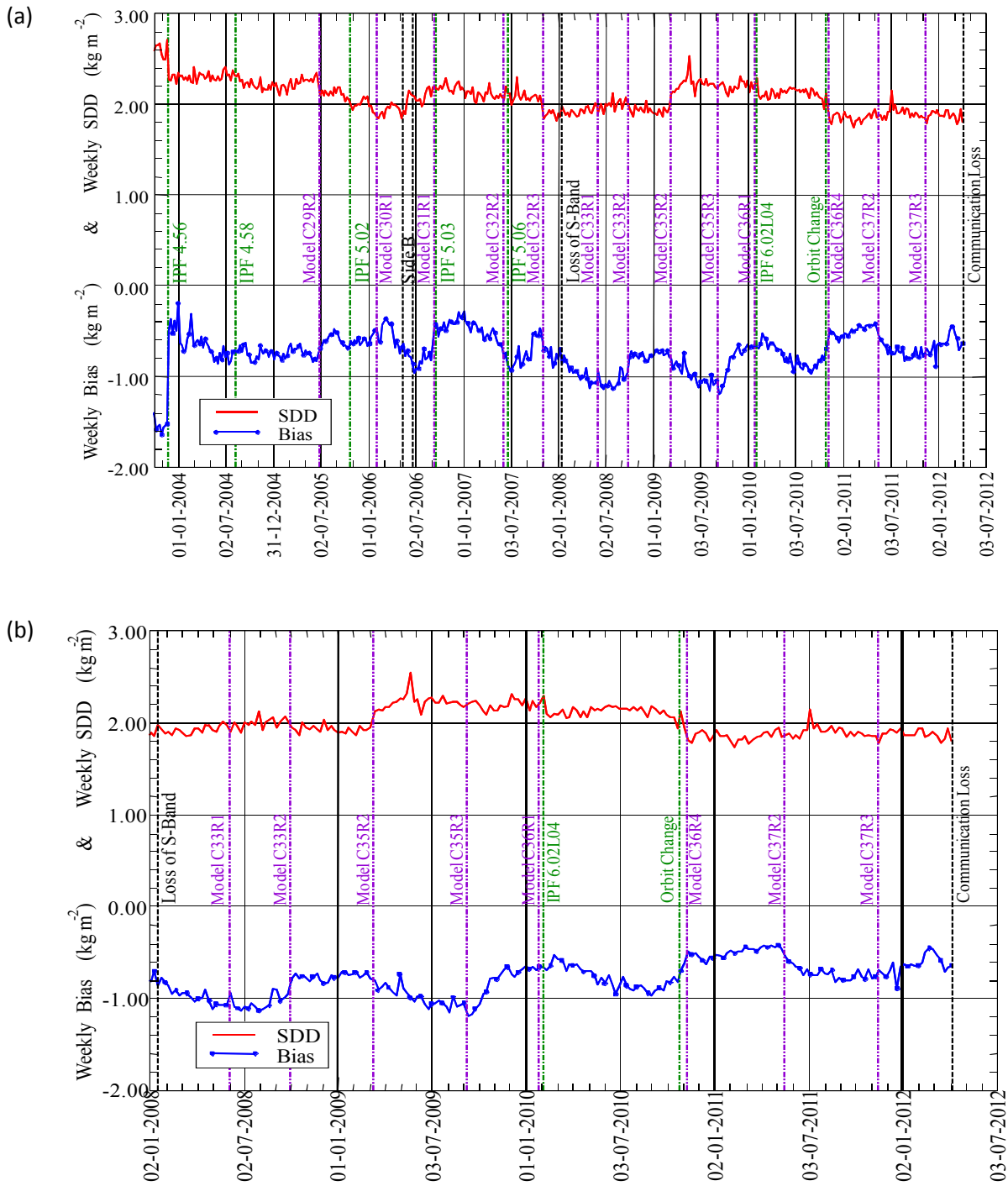


Figure I.11: Time series of weekly TCWV bias and standard deviation of difference between MWR and ECMWF model AN since late 2003 (a) and during the last 4 years (b).

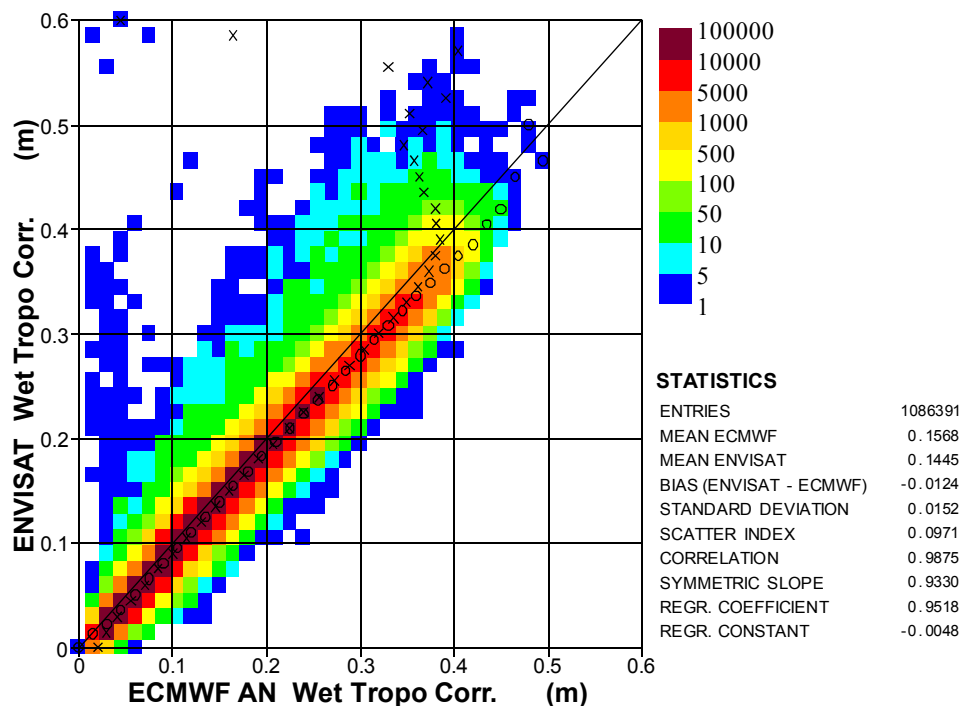


Figure I.12: Global comparison between MWR and ECMWF model AN WTC values during the period from 1 January 2011 to 31 December 2011.

involving model sea ice information were used in an attempt to eliminate most of those outliers. The WTC scatter plot in Fig. (I.12) shows one of the adverse impacts of the IPF 6.02L04 in a form of a secondary cloud of collocations running parallel to the main cloud with MWR values higher than the model. This cloud did not exist before the implementation of IPF6.02L04 (Abdalla, 2011). Investigations are being carried out to understand the possible reasons behind this.

The time series of weekly bias (MWR-model) and SDD between MWR and ECMWF model analysis WTC over the last few years is shown in panel (a) of Fig. (I.13). The same plot over the last 4 years is shown in panel (b) of Fig. (I.13). The MWR globally underestimates the WTC on average by about 12 mm compared to the model everywhere. The bias with respect to the model follows a seasonal cycle similar to that of TCWV. A slight degradation as a result of the implementation of IPF6.02L03 can be spotted as an increase of the SDD. This may be attributed mainly to the existence of the secondary cloud of collocations appeared in the scatter plot shown in Fig. (I.12). Apart from that, there is quite good resemblance between the WTC time series (Fig. I.13) and the TCWV ones (Fig. I.11). Therefore, the same conclusions can be drawn for WTC regarding the impact of the IPF (except for IPF6.02L04) and the model changes and the seasonal cycle.

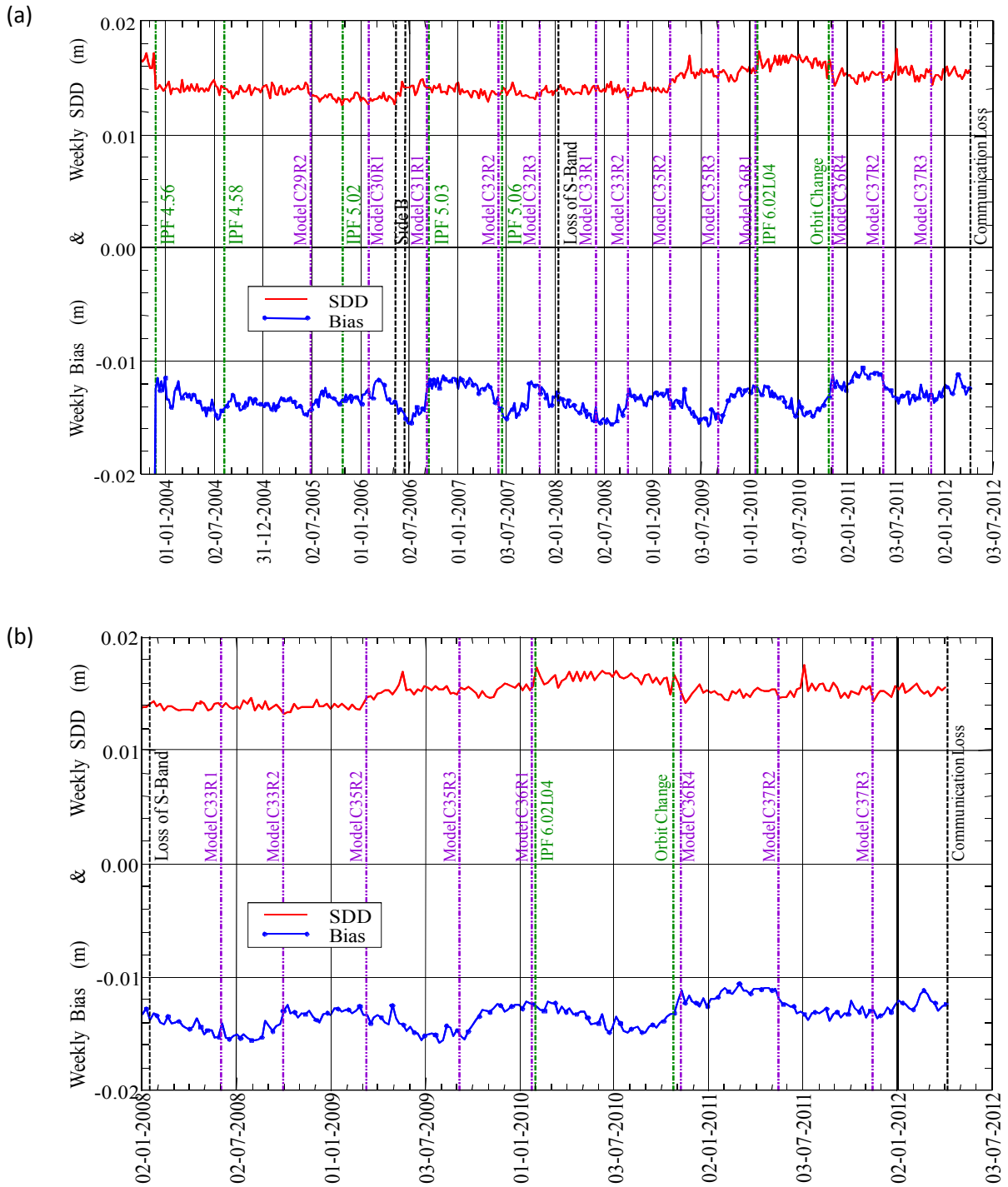


Figure I.13: Time series of weekly WTC bias and standard deviation of difference between MWR and ECMWF model AN since late 2003 (a) and during the last 4 years (b).

## I.8 Conclusions

Continuous monitoring and validation of the ENVISAT RA-2 wind and wave products together with the MWR water vapour products are carried out at ECMWF. Data from ECMWF atmospheric and wave models, from other satellites; namely: ERS-2 and Jason-1 and Jason-2, and from in-situ buoy and platform observations are used for this purpose.

The Ku-band backscatter coefficient has a rather stable monthly mean value. However, the monthly mean values were decreased by about 0.15 dB towards the end of 2009. About half of this reduction can be attributed to the change in IPF6.02L04 introduced in February 2010. Indeed, reduction of about the same amount was witnessed for Jason-1/2 altimeters. The S-band backscatter had few jumps due to processing changes before it was lost in January 2008. RA-2 wind speed data are in good agreement with the model and buoy data except for very high wind speeds (~21.4 m/s and above). This was corrected in the RA-2 processing chain IPF Version 6.02L04 (1 February 2010). Ku-band SWH product is of high quality. The absolute error in Ku-band SWH is about 6%. This is a low value compared to the other wave height observations available to us. The Ku-band SWH used to be too high by about 4.0% compared to the ECMWF model and the wave buoys before IPF 6.02L04 and virtually unbiased afterwards. There was also an increased standard deviation of the difference between the Ku-band SWH and the model after the implementation of IPF6.02L04. Ku-band SWH product has been assimilated in the ECMWF wave model since 22 October 2003.

The quality of the S-band wave height product used to be acceptable after some quality control procedure was used to filter out the RA-2 S-band Anomaly. Unfortunately, the S-band was permanently lost in January 2008.

The MWR products (TCWV and WTC) are stable during the last few years. Apart from a few outliers, the MWR products compare very well with the model. Most of the outliers can be attributed to ice and land contamination and can be filtered out using model information regarding the sea ice. In general, the MWR products are slightly drier than the model except for the Tropical TCWV. A group of outliers, with lower MWR values, that used to appear in the TCWV scatter plots, have disappeared after the implementation of the IPF6.02L04. Instead, a cloud of outliers (with higher MWR values) over most of the range of model values started to appear in the WTC scatter plots. This is still under investigation.

The change of ENVISAT orbit in October 2010 did not have any impact on RA-2 and MWR products except for a slight impact on the wind speed product for only few days just after the end of the manoeuvres.

## **II Advanced Synthetic Aperture Radar (ASAR) wave mode products**





## II.1 Introduction

ASAR consists of a coherent, active phased array SAR which is a distributed matrix of 320 transmitter/receiver elements operating at C-Band. The long axis of the SAR antenna is aligned in the direction of the satellite path (the azimuth direction). It images a strip of ground to the right side of the platform (range direction). The SAR produces two-dimensional representation of the scene reflectivity at high resolution. ASAR can operate in different modes but the Wave Mode is the one of interest here. In the wave mode, ASAR senses the changes in the backscatter from the ocean surface due to the action of long ocean waves. As a result it produces small images (of  $\sim 5$  km x 5km or larger) with 100 km spacing. This intermittent operation provides a low data rate so that the data can be stored on board the satellite and communicated whenever possible. The small images are then processed to produce the SAR cross-spectra (ASAR Wave Mode Level 1b, ASA\_WVS\_1P) product. Further processing produces the inverted ocean wave (ASAR Wave Mode Level 2, ASA\_WVW\_2P) product. In fact this latter step can be done offline using several other inversion methods. One method, which is used at ECMWF for the verification of Level 1b product, is the MPIM scheme developed by Hasselmann et al. (1996). ASAR Wave Mode products represent a unique opportunity to provide ocean wave spectra with global coverage. However, there are several limitations. The most important is the inability of the instrument to resolve high frequency (short) ocean wave components. The shortest resolvable wavelength is called the azimuthal cut-off.

## II.2 ASAR data processing

FD ASAR Wave Mode Level 1b (ASA\_WVS\_1P) and Level 2 (ASA\_WVW\_2P) products are validated. Level 1b product is the main product upon which basic quality control is done. Data processing is similar to the procedure used for ERS-2 SAR processing (see Abdalla and Hersbach, 2004). Here is a summary of this procedure:

The stream of ASAR product is split over 6-hour time windows centred at the main synoptic times to coincide with the model output times. The data contents of each time window is pre-processed to generate a list with output positions for the WAM model in order to produce a collocation file of wave spectra to be used for the SAR-inversion system. This includes basic pre-processing quality control checks to reject any spectrum with obvious anomalies and/or inconsistencies. The product parameters are checked and if any is found to be not logical, a quality control flag is set and the spectrum is rejected.

The nearest WAM wave spectra are extracted and used as the first guess (FG) to invert the ASAR product. The MPIM scheme (Hasselmann et al., 1996) which is an iterative method based on the forward closed integral transformation, is used for the inversion. During and after the iterative inverting procedure further quality checks are done. The iterations stop when there is a convergence (within a given tolerance) or until the iteration procedure starts to be unstable. The value of the final cost function (the lower the cost function the better the inverted spectrum is) and the stability of the procedure are used to define the quality of the final inverted spectrum.

Any Level 2 product is accepted only if the corresponding Level 1b product passes the quality control. Further quality checks are performed over accepted Level 2 products to ensure their consistency. Each quality controlled product is then collocated with the closest wave model spectrum. It should be noted that most of the comparisons (scatter plots and time series derived from those plots) between Level 2 product and the wave model are carried out within the spectral range resolvable by ASAR. Therefore, the part of the spectrum with wavelengths higher than the azimuthal cut-off length (as provided by the ASAR Level 2 product) is considered. This is different from the comparisons between ASAR Level 1b product and the wave model where the whole spectrum is considered. Therefore, one needs to be careful in drawing conclusions when inter-comparing both products.

Validation of wave spectra with large number (100's) of degrees of freedom is not a straight-forward task. Therefore, the validation is usually done in terms of a limited number of integrated parameters. Significant wave height (SWH), mean wave period (MWP), wave spectral peakedness factor of Goda (WPF), wave directional spread (WDS) and mean wave direction (MWD) are among the most commonly used. These parameters can be defined as:

1. Significant wave height (SWH),  $H_s$ , is defined as:

$$H_s = 4.0\sqrt{m_0}$$

where  $m_0$  is the “zeroth” moment of the wave spectrum. In general, the “ $n$ -th.” moment of the spectrum,  $m_n$ , is defined as:

$$m_n = \int d\theta \int df f^n F(f, \theta)$$

where  $F$  is the wave spectrum in frequency,  $f$ , - direction,  $\theta$ , space. The first integration is done over all directions while the second is usually carried out from frequency 0 to  $\infty$ . However, for the verification of Level 2 product, the frequency integration is limited up to the frequency corresponding to the azimuthal cut-off wavelength.

2. The mean wave period (MWP) based on the “-1 th.” moment ( $m_{-1}$ ),  $T_{-1}$ , is defined as:

$$T_{-1} = m_{-1} / m_0$$

where  $m_0$  and  $m_{-1}$  are the “zeroth” and the “-1 th.” Moments, respectively, of the wave spectrum with the “ $n$ -th.” moment, in general, is defined above.

3. The wave directional spread (MDS),  $\sigma$ , is defined as:

$$\sigma = \sqrt{2[1 - r_1(f)]}$$

$$r_1 = m_0^{-1} \int df \int d\theta F(f, \theta) \cos[\theta - \varphi(f)]$$

$$\varphi(f) = a \tan \left\{ \frac{\int d\theta F(f, \theta) \sin(\theta)}{\int d\theta F(f, \theta) \cos(\theta)} \right\}$$

4. The mean wave propagation direction (MWD),  $\varphi$ , is defined as:

$$\varphi = a \tan \left\{ \frac{\left[ \int df \int d\theta F(f, \theta) \sin(\theta) \right]}{\left[ \int df \int d\theta F(f, \theta) \cos(\theta) \right]} \right\}$$

5. The wave spectral peakedness factor of Goda, (WPF),  $Q_p$ , is defined as:

$$Q_p = 2m_0^{-2} \int d\theta \int df f F^2(f, \theta)$$

Voorrips et al. (2001) suggested the use of the narrowband equivalent wave height,  $H_{T_1, T_2}$ , between wave periods  $T_1$  and  $T_2$  defined as:

$$H_{T_1 T_2} = 4 \left\{ \int_{1/T_2}^{1/T_1} df \int d\theta F(f, \theta) \right\}^{1/2}$$

Typically, the wave period interval  $[T_1, T_2]$  is selected as 2 seconds (2-s wave-period interval equivalent wave height). This enables a more detailed validation in terms of a rather limited number of parameters.

### II.3 ASAR level 1B product

SWH is the most commonly used parameter for typical validation of ocean wave products. Fig. (II.1) shows a density scatter plot for globally collocated SWH pairs of inverted ASAR Wave Mode Level 1B and the analysis WAM wave model for the period of one year from 1 January to 31 December 2011. As can be seen in Fig. (II.1), the agreement between the ASAR and the model is quite good with ASAR slightly underestimating the wave heights. In general, the underestimation of ASAR for the SWH is about 15 cm while the scatter index is about 14%.

Fig. (II.2) shows a density scatter plot for globally collocated mean wave period (MWP) pairs of inverted ASAR WM Level 1B and the analysis WAM wave model for the period from 1 January to 31 December 2011. The agreement between the inverted ASAR and the model MWP is very good with virtually no bias and very small scatter index. Considering the various geographical areas (not shown), the bias is about 0.2 s and the SI is about 7% everywhere. There are few outliers with rather large differences between ASAR and the model. Those outliers are mainly near the coasts and therefore can be attributed to the land contamination.

Similarly, the globally collocated wave directional spread (WDS) pairs of inverted ASAR WM Level 1B and the analysis WAM wave model for the same period are plotted as a density scatter plot in Fig. (II.3). The agreement is quite good. Globally, the WDS is not biased with rather small scatter index value (~10%). Considering the various geographical areas (not shown), the bias is in general less than 0.5% of the mean while the SI varies between 8.6% (in the Tropics) and 11.2% in the SH.

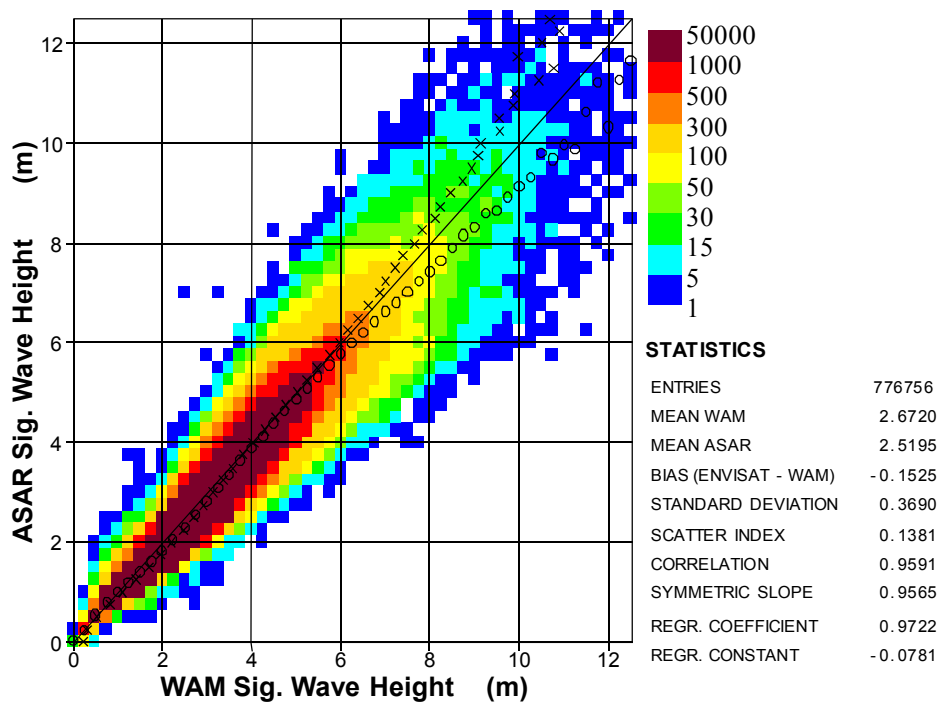


Figure II.1: Global comparison between inverted ASAR level 1b and ECMWF model SWH during the period from 1 January to 31 December 2011.

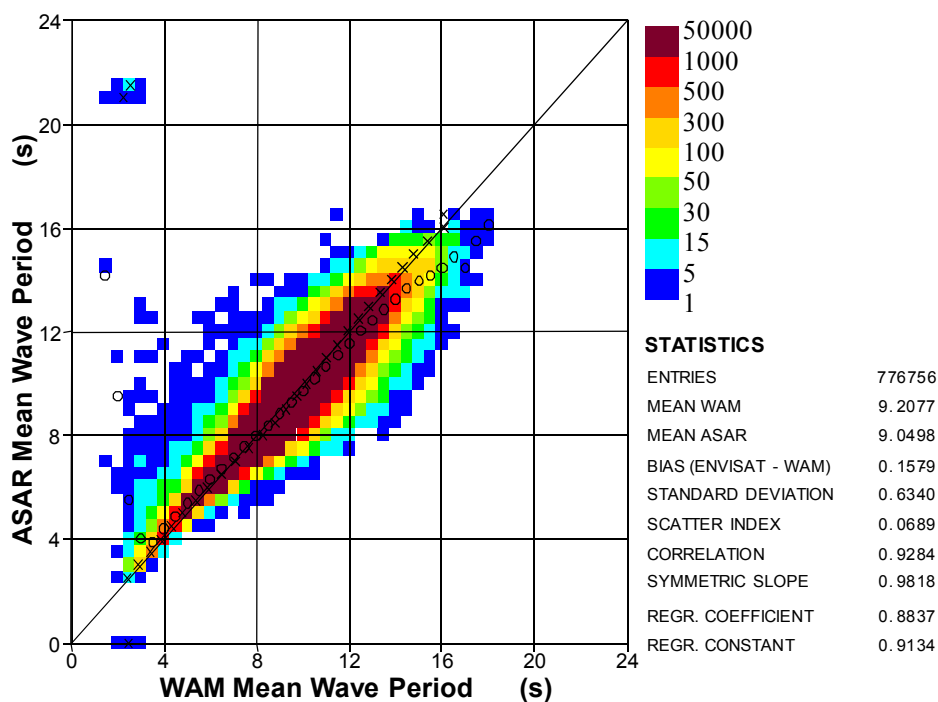


Figure II.2: Global comparison between inverted ASAR level 1b and ECMWF model MWP during the period from 1 January to 31 December 2011.

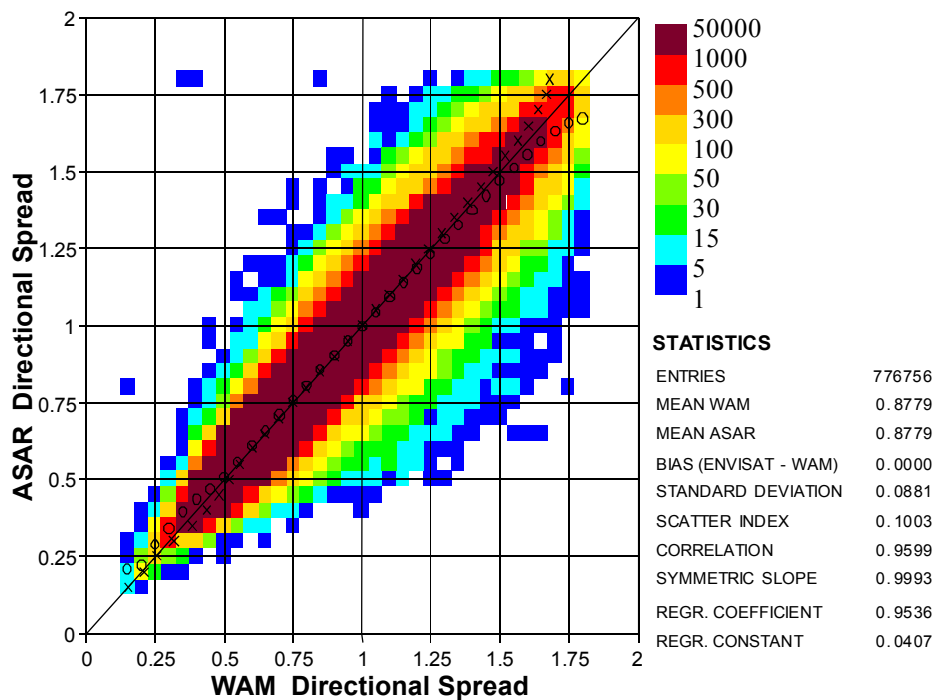


Figure II.3: Global comparison between inverted ASAR level 1b and ECMWF model WDS during the period from 1 January to 31 December 2011.

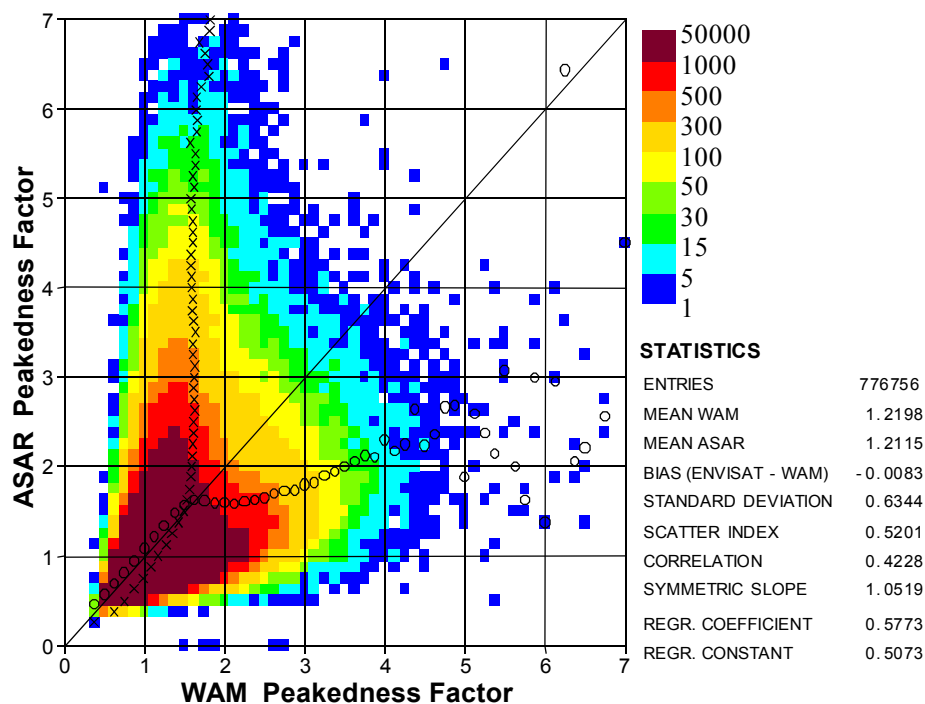


Figure II.4: Global comparison between inverted ASAR level 1b and ECMWF model WPF during the period from 1 January to 31 December 2011.

Globally collocated wave spectral peakedness factor (WPF) pairs of inverted ASAR WM Level 1B and the analysis WAM wave model for the whole year from 1 January to 31 December 2011 are plotted similarly in Fig. (II.4). There is a good agreement for most of the data, which have WPF values less than  $\sim 1.5$ . However, for larger peakedness factor values the agreement does not hold anymore with a clear split to form two families. The scatter index is rather high ( $\sim 50\%$ ) while the correlation coefficient is rather low ( $\sim 42\%$ ). Considering the various geographical areas (not shown), the bias is less than about 10% of the mean while the SI is about 43% in the Tropics and slightly above 50% in the extra-tropics.

## II.4 ASAR WM Level 2 product

It is stressed that the integrated parameters used here for the various comparisons are computed for the part of the spectrum which is resolvable by the ASAR instrument. This means that wave components with wavelengths longer than the azimuthal cut-off wavelength reported in the ASAR Wave Mode Level 2 (ASA\_WVW\_2P) product are used. The term swell is used for those parameters to reflect this fact (although strictly speaking is not correct).

Fig. (II.5) shows a density scatter plot for globally collocated swell SWH pairs of ASAR Wave Mode Level 2 and the analysis WAM wave model for a full year covering the period from 1 January to 31 December 2011. The agreement between the ASAR and the model is quite good for the bulk of the data. However, there are quite a number of outliers. The outliers are generally with higher ASAR values in the Tropics and with lower ASAR values in the SH (see Fig. II.12). The NH outliers are a combination of those in the Tropics and those in the SH. Globally, L2 product underestimates swell SWH by about 0.25 m. The scatter index is rather high with a global value of about 35%.

Similarly, Fig. (II.6) shows the density scatter plot for globally collocated swell mean wave period (MWP) pairs of ASAR Wave Mode Level 2 and the analysis WAM wave model for the full year of 2011. The agreement between the ASAR and the model MWP is very good for the bulk of the data. MWP is one of the parameters that definitely benefitted from the implementation of the processing chain of PF-ASAR 4.05 at the end of October 2007. On global scale, MWP is virtually unbiased. The global SDD of the mean wave period is about 0.5 s (less than 4%) which is quite good.

The globally collocated swell wave peakedness factor (WPF) pairs of ASAR Wave Mode Level 2 and the analysis WAM wave model for the same period are shown in Fig. (II.7) while the swell wave directional spread (WDS) pairs are shown in Fig. (II.8). The agreements between the ASAR WM L2 and the ECMWF wave model WPF and WDS are rather poor. The implementation of the processing chain of PF-ASAR 4.05 at the end of October 2007 slightly improved those parameters but not to the extent of promoting them to a level which can be described as “in good agreement” with the model. For example, the correlation between the L2 and model WPF is about 22% and for the WDS is about 34%. Fig.’s (II.7) and (II.8) suggest that the ASAR L2 spectra are very narrow both in frequency and direction compared to the model. This “narrowness” can be due to the physical restrictions on the SAR imaging process.

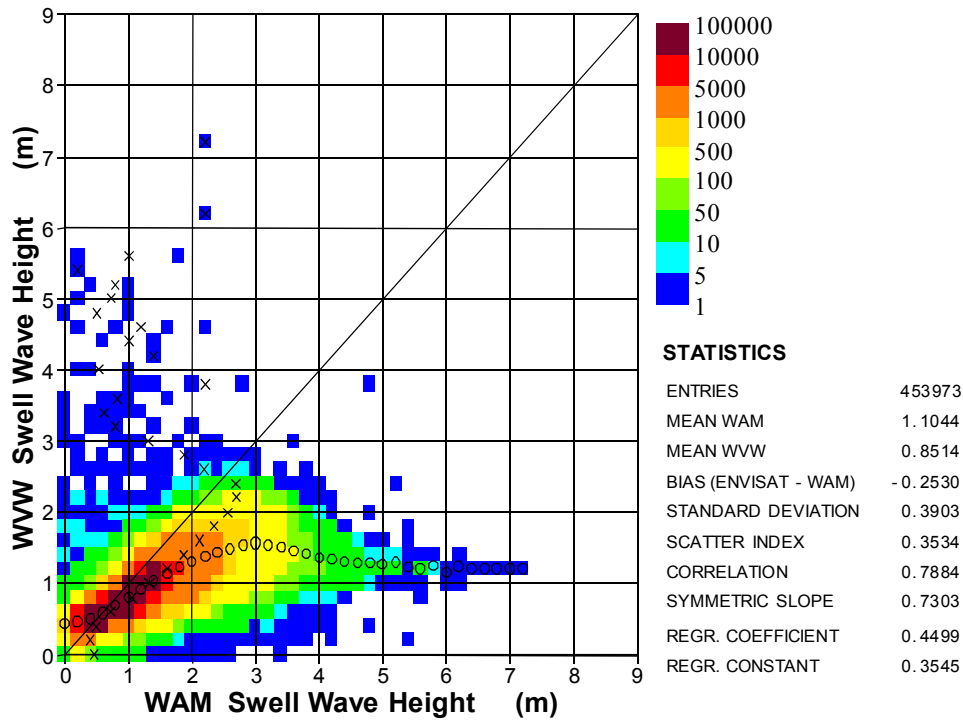


Figure II.5: Global comparison between ASAR level 2 and ECMWF model swell SWH (only within reported azimuthal cut-off) during the period from 1 January to 31 December 2011.

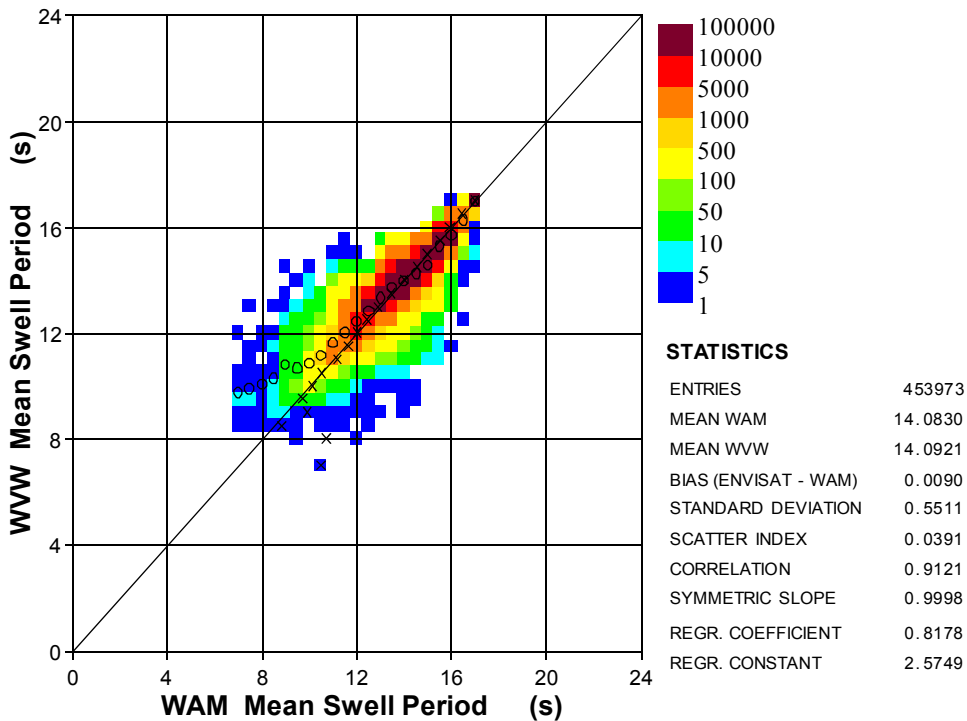


Figure II.6: Global comparison between ASAR level 2 and ECMWF model swell MWP (only within reported azimuthal cut-off) during the period from 1 January to 31 December 2011.

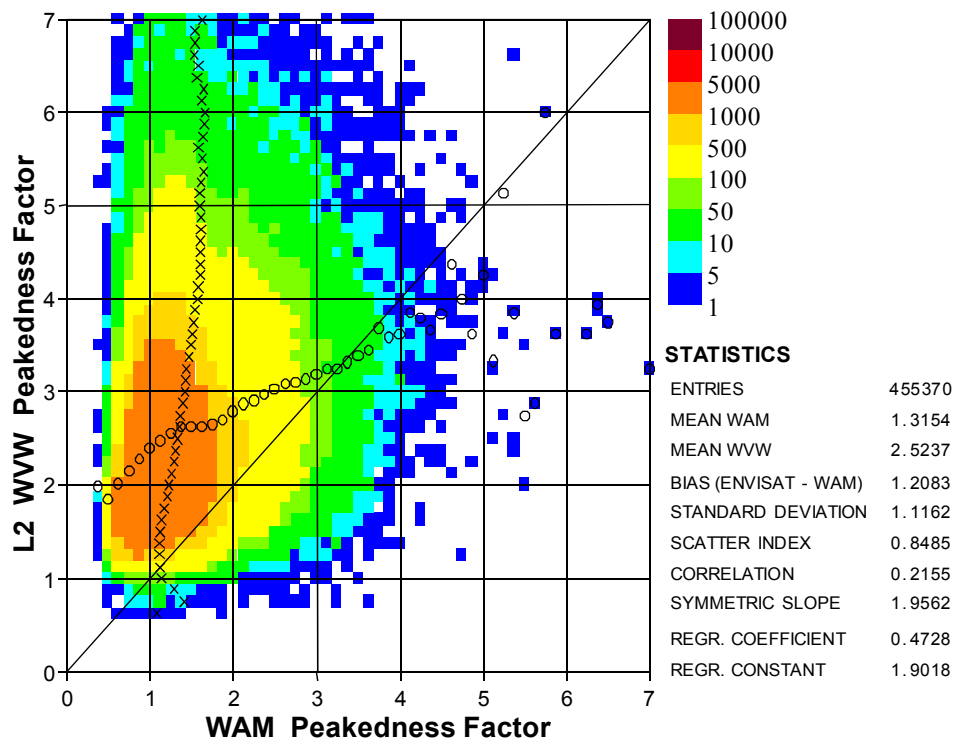


Figure II.7: Global comparison between ASAR level 2 and ECMWF model swell WPF during the period from 1 January to 31 December 2011.

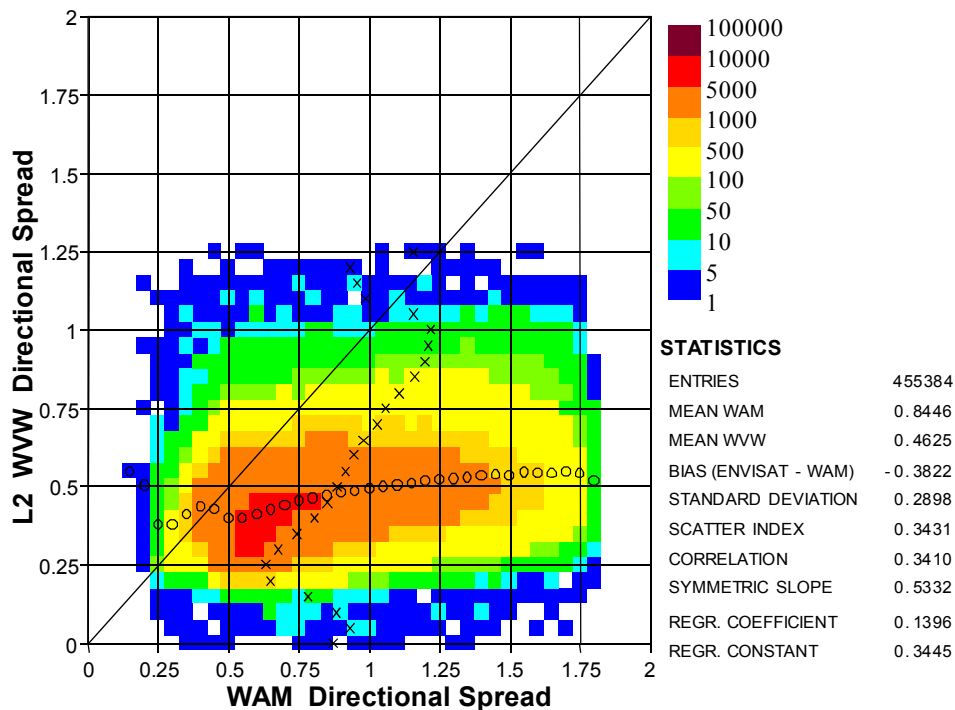


Figure II.8: Global comparison between ASAR level 2 and ECMWF model swell WDS during the period from 1 January to 31 December 2011.



## II.5 Assimilation of ASAR Wave Mode Level 2 product

Motivated by the change in ASAR processing chain of PF-ASAR 4.05 at the end of October 2007, Abdalla (2011) conducted several numerical experiments to test the impact of assimilating ASAR Wave Mode (WM) L2 ocean wave spectra product in the wave model of ECMWF. The model was run in a stand-alone mode (i.e. without coupling with the atmospheric part of IFS) with a configuration very close to the operational environment otherwise. Several quality control options were tested including the officially recommended ones as outlined by Johnsen (2005). Specifically, the following were found to give the best results:

- The sensed imagette is free from any land contamination by ensuring that *landFlag* is 0.
- The spectrum was inverted with enough confidence to produce an ambiguity-free spectrum. This is done by ensuring that the confidence parameter *confidence\_swell* is 0.
- Due to the absence of the “image normalized variance” (INV) parameter from the BUFR product, Abdalla (2011) used the signal-to-noise ratio (SNR) as another quality filter. Based on the recommendations of Aouf et al. (2008), SNR was limited to the range between 3 and 200.
- Only the sensed part of the spectrum, i.e. within a given cut-off wave length in azimuthal direction, is used. Therefore, a “cut-off ellipse” in the wave number vector space with a major axis extending over the whole wave number range in the range direction and a minor axis covering wave numbers within the given azimuthal cut-off in the azimuthal direction.
- Based on the recommendations of Aouf et al. (2008), assimilation was also limited to spectra associated with wind speeds in the range 3-16 m/s.

For those tests altimeter data were not assimilated to isolate the impact of ASAR assimilation. Further information regarding the experiment setup and data assimilation scheme can be found in Abdalla (2011) with some provided later here.

N. Miranda (2011, private communication), recommended the use of the “image normalized variance” (INV) parameter as a quality filter as it is thought to be an important filter to get rid of the questionable WM L2 spectra. To test this recommendation, the INV values were extracted from the original WM L2 PDS product and all spectra corresponding to INV values below 1.05 or above 1.5 were flagged as corrupt. This is done to avoid the complicated process of modifying the BUFR template.

A new set of experiments were carried out using updated model configuration to reflect the operational model changes. ECWAM model Cycle 38R1 (ECMWF operational IFS model cycle since 19 June 2012) was run in stand-alone mode (no coupling with the atmospheric part of IFS) for the period from 20 December 2011 to 8 April 2012. The first 12 days were discarded as a warm-up period and only the period from 1 January to 31 March was considered for analysis. The model was forced by operational wind fields. The globe was discretized into a grid with a resolution of about 28 km (0.25

degree) in both latitude and longitude directions. The spectral space was discretized into 36 frequency bins and 36 direction bins. The model was forced by operational wind fields. The analysis winds for 12 hours ending at 00 and 12 UTC each day were used. Data assimilation is carried out for the 6-hour windows centred at major synoptic times (i.e. at 00, 06, 12 and 18 UTC). This set-up resembles the configuration of the operational analysis. Further 5-day forecast without data assimilation follows the analyses at 00 and 12 UTC using operational forecast winds. Other details are similar to Abdalla (2011).

The main experiment made use of the ASAR L2 spectra flagged with the help of extracted INV values. Another experiment was carried out with the quality control that used by Abdalla (2011) which are similar to the main experiment except for the INV filter. A reference model run without any data assimilation was also carried out. Two other separate model runs were conducted by assimilating ASAR WM L1b data product in the first and RA-2 SWH data in the second. The altimeter data were not assimilated in any of the above experiments except for the RA-2 run mentioned above.

To assess the performance of each experiment, significant wave height data from Radar Altimeters on-board ENVISAT (RA-2) and Jason-1, ECMWF operational analysis and available ocean wave buoy and platform observations are used in the verification process as was carried out by Abdalla (2011). However, since the results are very similar to those shown by Abdalla (2011), only the in situ verification is shown here.

The impact of assimilating various ENVISAT products on error reduction of wave model analysis and forecast (FC) SWH in the Tropics as inferred from comparisons with in-situ measurements is shown in Fig. (II.9). Random error reduction is computed as:

$$\text{Error Reduction} = 100 * [ \text{SD}(\text{Hind-Buoy}) - \text{SD}(\text{Model-Buoy}) ] / \text{SD}(\text{Hind-Buoy}) \quad (1)$$

where SD is the standard deviation operator, Hind is the reference model hindcast without data assimilation, Model is the model run with data assimilation and Buoy is the collocated in situ measurement. This simple index describes the effectiveness of assimilated data in reducing the random model error compared to the case when no data is assimilated. Therefore, the higher the reduction value the more effective the data are.

It is clear that from Fig. (II.9) the assimilating ASAR WM L2 spectra filtered using INV values reduces the model error in the Tropics (between latitudes 20°N and 20°S) by about 2% at analysis time and decreases to less than 0.5% at day 5. This impact is about half of the impact due assimilating ASAR WM L1b which is, in turn, about half the impact due to assimilating RA-2. On the other hand, it is clear that filtering based on INV gives slightly better impact. When considering all available buoy observations which are mainly in the Northern Hemisphere (NH) including Tropics, the impact of data assimilation is limited and usually vanishes after 2-3 days. Fig. (II.10) shows that the ASAR impact is almost negligible at all FC lead times. The use of the INV filtering does not add to the results as the curve for the run without using it (not shown) coincides with the WM L2 curve.

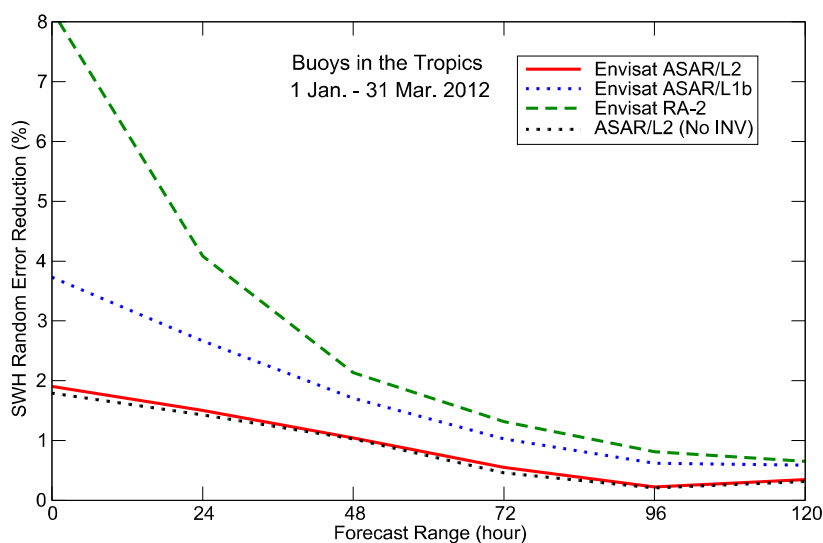


Figure II.9: Impact of assimilating ENVISAT ASAR WM L2 ocean wave product on error reduction of wave model analysis (plotted at FC range 0) and FC SWH as inferred from comparisons with in-situ measurements in the Tropics. For comparison, the impact of assimilating ASAR WM L1b and RA-2 SWH products are also shown together with the impact from ASAR WM L2 without the INV quality filtering.

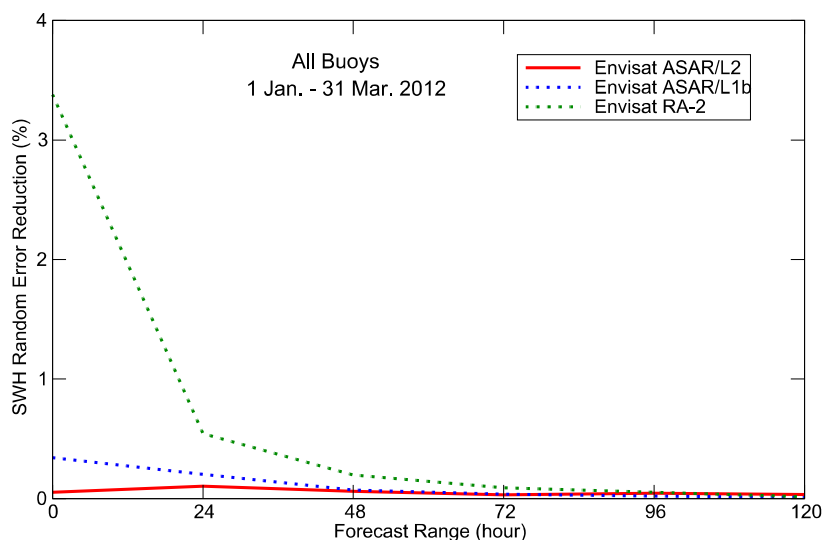


Figure II.10: Same as Fig. (II.9) but for all available buoys (mainly in the NH and Tropics).

Another important wave parameter which can be used to assess the impact of data assimilation is the peak wave period ( $T_p$ ). The peak wave period is defined as the wave period corresponding to the peak of the 1-D wave frequency spectrum. Several buoys report this parameter. Fig. (II.11) shows the impact of data assimilation on the reduction of peak wave period error as defined in Eq. (1). It comes as a surprise that assimilating the WM L2 product has a negative impact on the model analysis and FC during the first two days. It recovers only beyond day 2 when apparently the impact on the wave energy distribution vanishes (related to wave period) while the impact on the level of wave energy (related to wave height) remains. The use of the INV filtering does not add much to the results as can be seen in Fig. (II.11). It is interesting to see that at analysis time, assimilating WM L1b reduces the

peak wave period error by about 3.5% while assimilating RA-2 reduces the wave period error by more than 6%.

When considering all in situ measurements to assess the impact of assimilation, ASAR WM L2 has a negative impact on the peak wave period at analysis time as well as during the whole 5-day FC period as can be seen in Fig. (II.12). Using the INV filtering does not help in alleviating this negative impact.

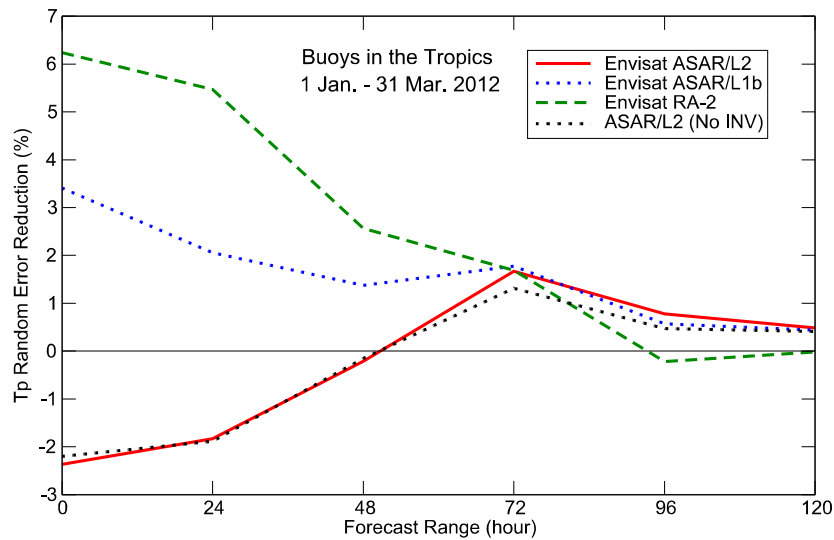


Figure II.11: Same as Fig. (II.9) but for the peak wave period in the Tropics.

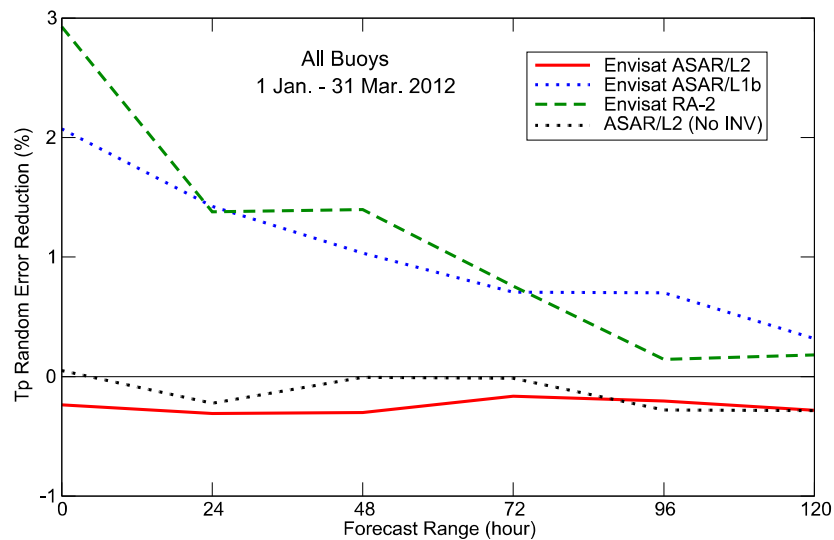


Figure II.12: Same as Fig. (II.11) but for all available buoys (mainly in the NH and Tropics).

## II.6 Conclusions

Continuous monitoring and validation of the ENVISAT ASAR Wave Mode products are carried out at ECMWF. Data from ECMWF wave model are used for this purpose. Improvements to the ASAR processing chain (PF-ASAR) are carried from time to time. PF-ASAR Ver. 4.05, in October 2007, is one of the important improvements.

ASAR Wave Mode Level 1b spectra are inverted using the MPIM scheme at ECMWF and have been assimilated since February 2006. The inverted ocean wave spectra compare well against the wave model products in terms of a limited number of integrated parameters although the comparison may not be very good as far as the details are concerned.

The comparison between ASAR Wave Mode Level 2 and the wave model is done in terms of the same integrated parameters with the exception that the integration is done for the ASAR resolvable wave components (i.e. with wavelengths longer than the azimuthal cut-off wavelength). Swell significant wave height and mean wave period from Level 2 product agree well with their wave model counterparts. However, the swell spectral peakedness factor and the directional spread parameters show poor agreement.

The change of ENVISAT orbit in October 2010 did not have any impact on ASAR Wave Mode products. The possible assimilation of ASAR WM Level 2 Product into ECMWF wave model was assessed. It seems that ASAR WM L2 product needs some improvements and/or the QC procedure needs some extra considerations to ensure the success of ASAR data assimilation (Abdalla, 2011). The use of the Image Normalised Variance (INV) parameter slightly improves the results but is not able to alleviate all the negative impact.

The change of the ASAR instrument configuration at various stages during the last two years (before the loss of the spacecraft) does not seem to have any impact on the quality of the ASAR disseminated products.



## **III Medium Resolution Imaging Spectrometer (MERIS) Water vapour product**





### III.1 Introduction

MERIS is a 68.5° field-of-view pushbroom imaging spectrometer that measures the solar radiation reflected by the Earth, at a ground spatial resolution of 300m, in 15 spectral bands, programmable in width and position, in the visible and near infra-red. MERIS allows global coverage of the Earth in 3 days. The MERIS product of interest is the Geolocated Cloud Optical Thickness and Water Vapour Content (a low resolution atmosphere Level 2) product (MER\_LRC\_2P). Specifically, only TCWV is validated here. This is a very dense product with a 1200 km wide swath at a resolution of 4.16 km (across-track) × 4.64 km (along-track) at nadir.

### III.2 MERIS data processing for monitoring

TCWV (or the “atmospheric water vapour content”) is one of the products obtained from the MERIS instrument onboard ENVISAT (product MER\_LRC\_2). This product is validated by comparing it with the corresponding product produced by the ECMWF atmospheric model (IFS). Due to the scale differences between the MERIS product and the IFS model product, it is required to bring both to the same scale. One way to do this is to average the MERIS product over spatial grid boxes comparable with the model resolution. A procedure for the pre-processing including the averaging and the basic quality control can be summarised as follows (Abdalla, 2005):

1. The stream of MERIS MER\_LRC\_2 product is split over 6-hour time windows centred at the main synoptic times to coincide with the IFS model output times.
2. All MERIS TCWV observations with missing or zero values are filtered out assuming they are not valid.
3. For each time window, the dense MERIS TCWV data set is averaged over grid boxes of 0.5°×0.5° producing the MERIS super-observations.
4. The super-observation is rejected if the number of its individual observations is less than 10.
5. The super-observation is rejected if it is smaller than 0.1 kg/m<sup>2</sup>.
6. The super-observation is rejected if its standard deviation exceeds 35% of its mean.
7. The super-observations that pass the quality control are collocated with the model counterparts and various statistics are computed.

This procedure may reject more than 40% of MERIS TCWV products. It is important to stress that part of the rejected data may be of good quality and rejected due to their high variability

### III.3 MERIS Water vapour product

Fig. (III.1) shows a time series of monthly mean MERIS TCWV data reception and acceptance per 6-hour time window since the mid of 2005. On average, the data received at a rate exceeding 3 million observations per 6-hours. Before the implementation of the MERIS processing chain IPF 5.02 (May 2006), about 50% of the received data pass the quality control. This is already a rather low ratio. The IPF 5.02 lead to more rejections and brought the ratio to about 70%. It is not clear if this low ratio is due to the noise/variability in the observations or due to the current quality control procedure which was derived based on the results of an optimisation of the data acceptance against the best agreement with respect to the model (c.f. Abdalla, 2005).

Collocated TCWV pairs of MERIS super-observations and the ECMWF model AN are plotted as density scatter plot in Fig. (III.2) for the whole globe over a full year period from 1 January - 31 December 2011 (panel a). The corresponding plot for the year 2009 is given in panel (b) of Fig. (III.2) for comparison. The major part of the MERIS observations agrees very well with the model counterpart. However, MERIS TCWV tends to provide, as can be seen in Fig. (III.2), a significant number of dry observations especially below  $\sim 15\text{-}20\text{ kg/m}^2$  which are not supported by the model. As a result, MERIS tends to have a secondary population of collocations with the model that runs below the main population by  $\sim 10\text{ kg/m}^2$ . Although this cannot be clearly seen in Fig. (III.2), it is very pronounced in scatter plots of shorter time spans, e.g. monthly, and particularly in the Tropics (not shown).

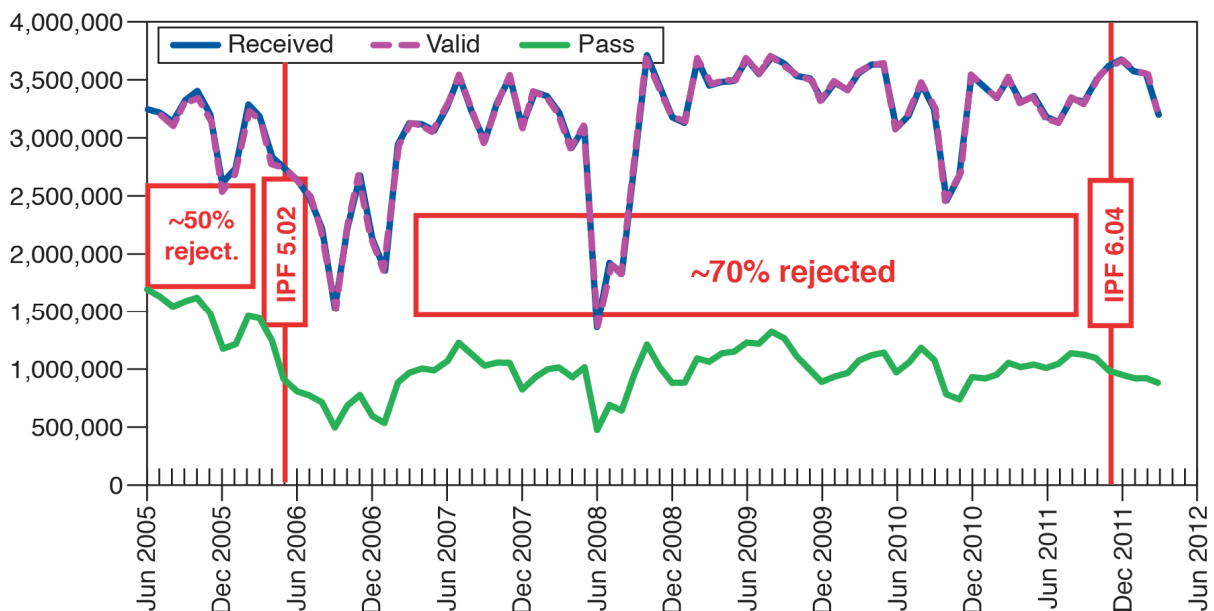


Figure III.1: Time series of monthly mean MERIS TCWV data reception and acceptance per 6-hour window.

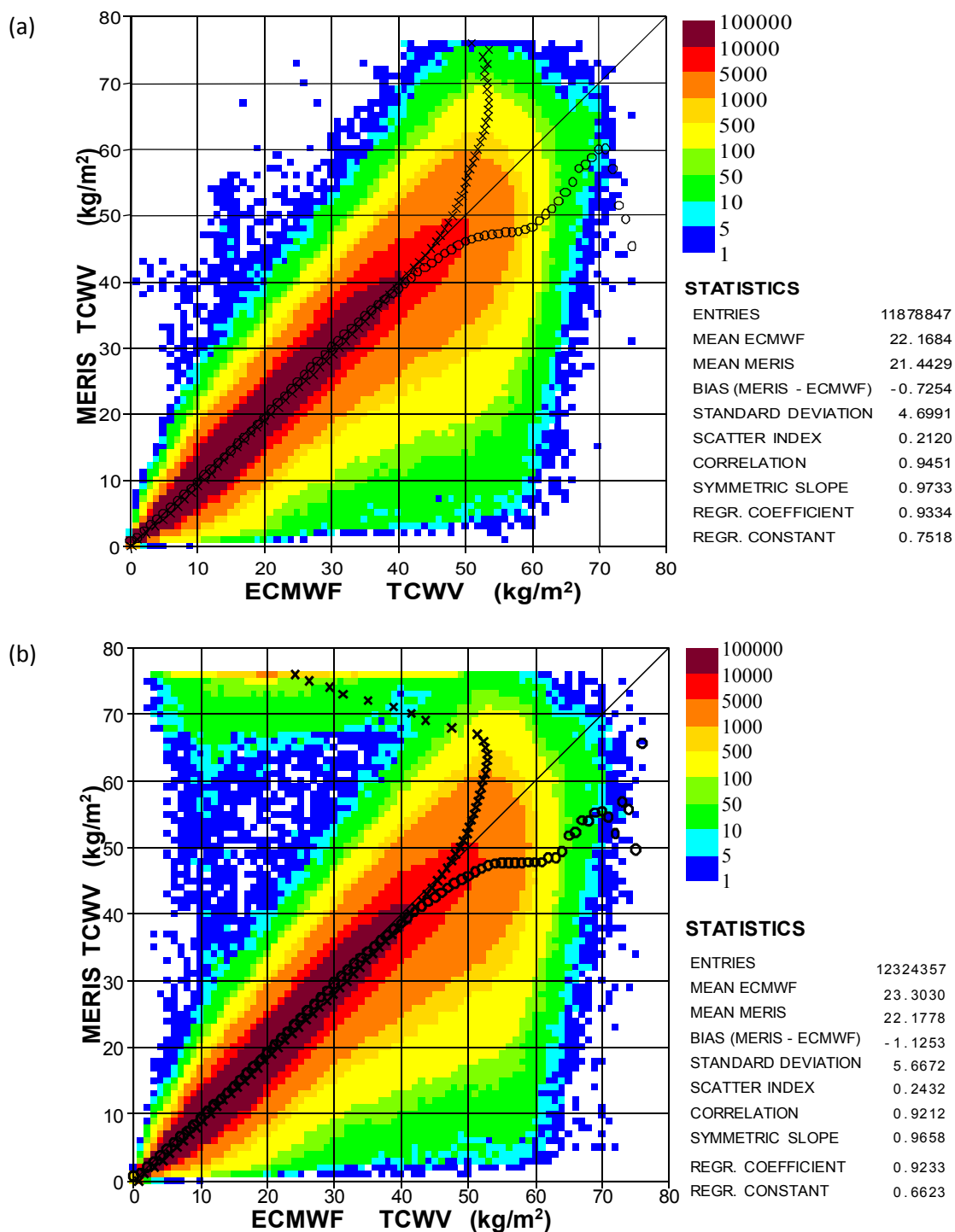


Figure III.2: Global comparison between MERIS and ECMWF model AN TCWV values during periods: (a) from 1 January - 31 December 2011 and (b) from 1 January - 31 December 2009 (for comparison).

On 3 November 2011, the MERIS IPF Version 6.04 was operational. The change list includes, among others, a new algorithm for water vapour retrieval over land. For the details, refer to:

<http://envisat.esa.int/earth/www/object/index.cfm?fobjectid=8018> and  
<http://envisat.esa.int/earth/www/object/index.cfm?fobjectid=8052>.

Globally over the whole year of 2011, MERIS underestimates the TCWV by about 0.7 kg/m<sup>2</sup> with respect to the ECMWF atmospheric model (panel a of Fig. III.2). As can be seen in panel (b) of Fig. (III.2), for example, typically, this value used to be about 1 kg/m<sup>2</sup> before the implementation of MERIS IPF 6.04 on 3 November 2011. The current monthly global value is around 0.1 kg/m<sup>2</sup>. The current scatter index (about 21%) is also smaller than before. Note that the difference suggested in both panels of Fig. (III.2) suffers from slight exaggeration due to the existence of the outliers with abnormal differences (in excess of ~70 kg/m<sup>2</sup>) resulted from the experimentation with the MERIS instrument at various short periods during 2009.

The time series of the bias (MERIS – model) and the standard deviation of difference (SDD) are plotted in Fig. (III.3). Global statistics and those at various geographical hemispheres (latitudes 20°N and 20°S are used as the boundaries for those regions. It is clear that the bias during November and December 2011 is closer to the zero bias compared to the values from the same period in the previous two years. These two months also show the lowest SDD values compared to same period from 2010 and 2009.

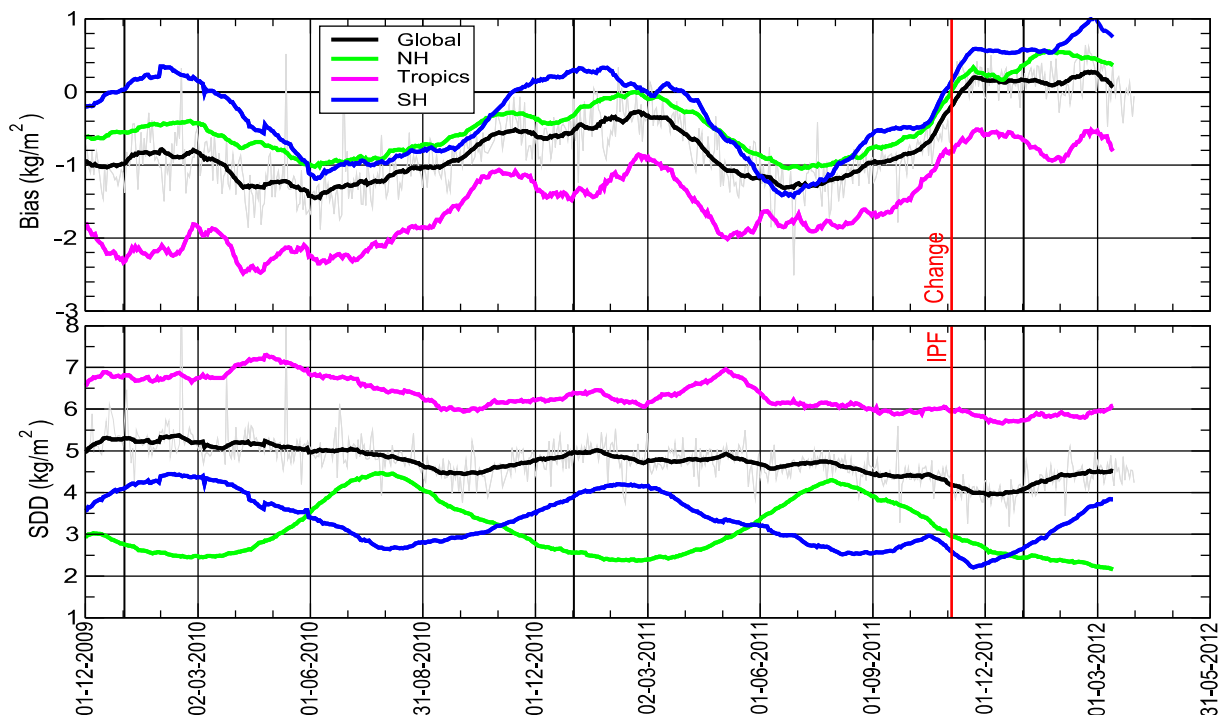


Figure III.3: Time series of global bias and SDD between MERIS and ECMWF model.

### **III.4 Assimilation of MERIS TCWV**

The fact that there is not much water vapour data over land and the result presented above that MERIS TCWV data are good over land motivated the satellite group at ECMWF to make experiments to test the impact of assimilating MERIS TCWV over land only. They needed to create super-observations comparable with the model resolution and to introduce some screening and quality control (QC) criteria. They also needed to do analysis of the spatial correlation. They found that the results were in general rather neutral compared to the model. However, some positive (and consistent with microwave measurements) impact against radiosondes was noticed. For details, refer to Bauer (2009). Finally, MERIS TCWV product over land has been assimilated with VarBC operationally since 8 September 2009.

### **III.5 Conclusions**

MERIS TCWV product shows that there is quite a good value in the product especially over land. Careful data screening is needed to get rid of the “noise”, which may also be a legitimate variability, in the data. This leads to the rejection of about 70% of the data. The product in general is too dry compared to the model. However, it is at a comparable level of dryness as the MWR. Although the product is averaged to form the super-observations which, in principle, should smooth the product and make it of comparable scale like the model, it is still too “noisy” when compared to the model or the MWR.

Being of better performance over land where not many alternative data are available, MERIS TCWV product has been assimilated operationally in the ECMWF atmospheric model since 8 September 2009.

The change of ENVISAT orbit in October 2010 did not have any impact on MERIS water vapour product.

The operational implementation of MERIS IPF Version 6.04 on 3 November 2011, resulted in slightly better TCWV product.

## Acknowledgments

This work was carried out with ESA support through various ESA contracts (under the title of Global Validation of ENVISAT Data Products). Special thanks are due to Peter Janssen and Jean-Raymond Bidlot for support and valuable discussion.

## References

- Abdalla, S. (2005). Global Validation of ENVISAT Wind, Wave and Water Vapour Products from RA-2, MWR, ASAR and MERIS. *Final Report for ESA contract 17585*. Available online at: <http://www.ecmwf.int/publications/library/do/references/show?id=86908>
- Abdalla, S. (2011). Global Validation of ENVISAT Wind, Wave and Water Vapour Products from RA-2, MWR, ASAR and MERIS (2008-2010). *Final Report for ESA contract 21519/08/I-OL*. Available online at: <http://www.ecmwf.int/publications/library/do/references/show?id=90046>
- Abdalla, S. and Hersbach, H. (2004). The technical support for global validation of ERS Wind and Wave Products at ECMWF. *Final Report for ESA contract 15988/02/I-LG*. Available online at: <http://www.ecmwf.int/publications/library/do/references/show?id=86313>
- Aouf, L., Lefèvre, J-M., Chapron, B. and Hauser, D. (2008). Some recent improvements of the assimilation of upgraded ASAR L2 wave spectra”, *SeaSAR 2008, ESA Workshop*, Frascati, Italy, 21-25 January 2008.
- Bauer, P. (2009); 4D-Var assimilation of MERIS total column water-vapour retrievals over land, *Quart. J. Royal Meteor. Soc.*; **135**; 1852-1862
- Hasselmann, S., Bruning, C., Hasselmann, K. and Heimbach, P. (1996). An Improved Algorithm for the Retrieval of Ocean Wave Spectra from Synthetic Aperture Radar Image Spectra. *J. of Geophysical Research*, **101**, 16615-16629.
- Johnsen, H. (2005). Envisat ASAR Wave Mode Product Description and Reconstruction Procedure. *Report for ESA Contract 17376/03/I-OL*.
- Voorrips, A.C., Mastenbroek, C. and Hansen, B. (2001). Validation of two algorithms to retrieve ocean wave spectra from ERS synthetic aperture radar. *J. of Geophysical Research*, **106**, 16825-16840.